Available online at www.sciencedirect.com

SciVerse ScienceDirect

Geochimica et Cosmochimica Acta 95 (2012) 143–159

Geochimica et Cosmochimica Acta

www.elsevier.com/locate/gca

Degradation of terrestrial organic carbon, primary production and out-gassing of CO_2 in the Laptev and East Siberian Seas as inferred from $\delta^{13}C$ values of DIC

V. Alling [a,b,*], D. Porcelli [c], C.-M. Mörth [b,d,e], L.G. Anderson [f], L. Sanchez-Garcia [a,b], Ö. Gustafsson [a,b], P.S. Andersson [g], C. Humborg [a,b,e]

[a] Dept. Applied Environmental Sci., Stockholm University, Sweden
[b] Bert Bolin Centre for Climate Research, Stockholm University, Sweden
[c] Dept. Earth Sci., Oxford University, UK
[d] Dept. Geological Sci., Stockholm University, Stockholm, Sweden
[e] Baltic Nest Institute, Stockholm University, Sweden
[f] Dept. Chem., University of Gothenburg, Gothenburg, Sweden
[g] The Swedish Museum of Natural History, Stockholm, Sweden

Received 9 May 2011; accepted in revised form 23 July 2012

Abstract

The cycling of carbon on the Arctic shelves, including outgassing of CO_2 to the atmosphere, is not clearly understood. Degradation of terrestrial organic carbon (OC_{ter}) has recently been shown to be pronounced over the East Siberian Arctic Shelf (ESAS), i.e. the Laptev and East Siberian Seas, producing dissolved inorganic carbon (DIC). To further explore the processes affecting DIC, an extensive suite of shelf water samples were collected during the summer of 2008, and assessed for the stable carbon isotopic composition of DIC ($\delta^{13}C_{DIC}$). The $\delta^{13}C_{DIC}$ values varied between $-7.2‰$ to $+1.6‰$ and strongly deviated from the compositions expected from only mixing between river water and seawater. Model calculations suggest that the major processes causing these deviations from conservative mixing were addition of (DIC) by degradation of OC_{ter}, removal of DIC during primary production, and outgassing of CO_2. All waters below the halocline in the ESAS had $\delta^{13}C_{DIC}$ values that appear to reflect mixing of river water and seawater combined with additions of on average 70 ± 20 μM of DIC, originating from degradation of OC_{ter} in the coastal water column. This is of the same magnitude as the recently reported deficits of DOC_{ter} and POC_{ter} for the same waters. The surface waters in the East Siberian Sea had higher $\delta^{13}C_{DIC}$ values and lower DIC concentrations than expected from conservative mixing, consistent with additions of DIC from degradation of OC_{ter} and outgassing of CO_2. The outgassing of CO_2 was equal to loss of 123 ± 50 μM DIC. Depleted $\delta^{13}C_{POC}$ values of $-29‰$ to $-32‰$ in the mid to outer shelf regions are consistent with POC from phytoplankton production. The low $\delta^{13}C_{POC}$ values are likely due to low $\delta^{13}C_{DIC}$ of precursor DIC, which is due to degradation of OC_{ter}, rather than reflecting terrestrial input compositions. Overall, the $\delta^{13}C_{DIC}$ values confirm recent suggestions of substantial degradation of OC_{ter} over the ESAS, and further show that a large part of the CO_2 produced from degradation has been outgassed to the atmosphere.

1. INTRODUCTION

The processes affecting the remobilization, transport and fate of terrestrial organic carbon (OC_{ter}) in the Arctic are attracting increasing attention because of the potentially

* Corresponding author. Present address: Norwegian Geotechnical Institute, Norway.
E-mail address: vanja.alling@ngi.no (V. Alling).

0016-7037/$ - see front matter © 2012 Elsevier Ltd. All rights reserved.
http://dx.doi.org/10.1016/j.gca.2012.07.028

huge effect a warmer climate might have on carbon dynamics in this region (e.g. McGuire et al., 2009). In the Northern hemisphere, a major reservoir of terrestrial organic carbon is found in permafrost, which stores 30–50% of the world's soil carbon (Tarnocai et al., 2009). Arctic rivers draining these regions are responsible for a major flux of C to the ocean, transporting more than 10% of the global riverine freshwater and terrestrial organic carbon into the Arctic Ocean (Dittmar and Kattner, 2003). Concerns have been raised about increasing global warming caused by the CO_2 produced by degradation of OC_{ter} when permafrost thaws (e.g. Guo and MacDonald, 2006; Frey and McClelland, 2009; McGuire et al., 2009).

The Lena River has the highest annual organic carbon discharge in the Arctic (Raymond et al., 2007). It has a very large and wide spread impact on the East Siberian Arctic Shelf Seas (ESAS), i.e. the Laptev and East Siberian Seas (Semiletov et al., 2005), which constitute 40% of the total Arctic shelf (Jakobsson et al., 2008). In recent studies, terrestrial organic matter transported to the ESAS has been shown to be subject to significant degradation across the shelf, as inferred from the levels of pCO_2 oversaturation (Semiletov et al., 2007; Anderson et al., 2009), removal fluxes of both terrestrial dissolved organic carbon (DOC_{ter}) (Manizza et al., 2009; Alling et al., 2010; Letscher et al., 2011), and particulate organic carbon (POC_{ter}) (Sanchez-Garcia et al., 2011) and from the molecule-specific $\delta^{13}C$–$\Delta^{14}C$ trends in POC across the shelf (van Dongen et al., 2008; Vonk et al., 2010). This degradation of OC_{ter} results in an excess of dissolved inorganic carbon (DIC) that might be outgassed as CO_2. However, some of the DIC may also be used by primary producers, and instead be converted back to organic carbon. Since there are several sources and sinks for DIC, the extent to which each of these different processes affects the DIC system cannot be inferred from DIC concentrations alone.

The effects of degradation of OC_{ter} to DIC, assimilation of DIC by primary production and outgassing of CO_2 could be more easily distinguished from one another by combining the DIC concentration measurements with $^{13}C/^{12}C$ isotope ratios, generally reported as $\delta^{13}C_{DIC}$ values. Isotopes also have the advantage of integrating information regarding the extent of losses and additions that have occurred and are not clearly seen in a synoptic survey of the distribution of concentrations of dissolved and particulate constituents at one time. Losses of DIC generally leave isotopically heavy C, although the extent of isotope fractionation is different between losses by outgassing of CO_2 and by primary production (Mook et al., 1974; Zeebe and Wolf-Gladrow, 2001). Erlenkeuser et al. (2003) used $\delta^{13}C_{DIC}$ values to show the influence of primary production on DIC concentrations in the Kara Sea. Addition of DIC by degradation of OC_{ter} has the opposite effect by adding isotopically light C. Therefore, the relative changes in DIC concentrations and $\delta^{13}C_{DIC}$ leave unique fingerprints in the water. The general behavior and isotopic composition systematics of DIC have been extensively discussed in Zeebe and Wolf-Gladrow (2001).

There are few studies on primary production rates in the Laptev Sea and none for the East Siberian Sea, although models have suggested it is the same range for both areas (Stein and Macdonald, 2004; Pabi et al., 2008). The DOC and POC inventories investigated during the International Siberian Shelf Study 2008 (ISSS-08; Semiletov and Gustafsson, 2009) have been recently described (Alling et al., 2010; Sanchez-Garcia et al., 2011). The present study focuses on the connection between the organic and inorganic carbon cycles to better understand carbon cycling in the ESAS water column and in particular the sources and sinks of DIC. We have extended the approach of Erlenkeuser et al. (2003) and applied it to the ESAS to show that the $\delta^{13}C_{DIC}$ values can also be used to identify the effects of other processes affecting the carbon cycling in the low salinity mixing zones on the shelf. This was done by collecting samples for $\delta^{13}C_{DIC}$ from waters across the region, extending from the Lena River mouth to the outer shelf of the East Siberian Sea and combining those values with the concentrations of DIC (Anderson et al., 2009). Comparison between the data and model calculations of the major processes affecting DIC, reveal the relative impact of degradation of OC_{ter}, $CaCO_3$ dissolution, primary production and outgassing of CO_2 on the carbon system. The overall roles of the various regions within the ESAS as sinks or sources for DIC, and so for atmospheric CO_2, could therefore be identified.

2. METHODS

2.1. Study area

Sampling was conducted during the International Siberian Shelf Study 2008 (ISSS-08) cruise on the Russian RV Yacob Smirinsky, along the East Siberian Arctic Shelf (ESAS), which included the Lena River estuary in the Laptev Sea, the eastward branch of the Lena River plume extending into the East Siberian Sea, and the Pacific-influenced waters of the eastern East Siberian Sea (see Fig. 1). The Laptev Sea is situated between ~110°E (Severnaya Zemlya) and 140°E (the New Siberian Islands). It covers almost 5×10^5 km^2 and has an average water depth of 50 m (Jakobsson et al., 2004). The Laptev Sea receives freshwater discharge (~ 745 km^3 year^{-1}) mainly from the Lena River (566 km^3 year^{-1}) (Cooper et al., 2008). The East Siberian Sea, with an average water depth of 58 m, is the largest, the most ice-bound, and the least explored of the Arctic marginal seas (Stein and Macdonald, 2004). It covers an area of 9.9×10^5 km^2 stretching from 140°E to 180°E. There are two major rivers entering into the East Siberian Sea, the Indigirka (152°E) and the Kolyma (162°E), with annual discharges of 61 and 114 km^3 year^{-1}, respectively (Cooper et al., 2008).

The circulation patterns of the ESAS, as well as freshwater residence times, are described in detail elsewhere (Steele and Ermold, 2004; Semiletov et al., 2005; Alling et al., 2010). The coastal currents along the Laptev and East Siberian Seas flow predominantly eastwards. The Lena River discharges into the Laptev Sea resulting in a pronounced plume extending northward. A major, but poorly quantified, proportion of the freshwater discharge from the Lena River is transported by the coastal currents eastward

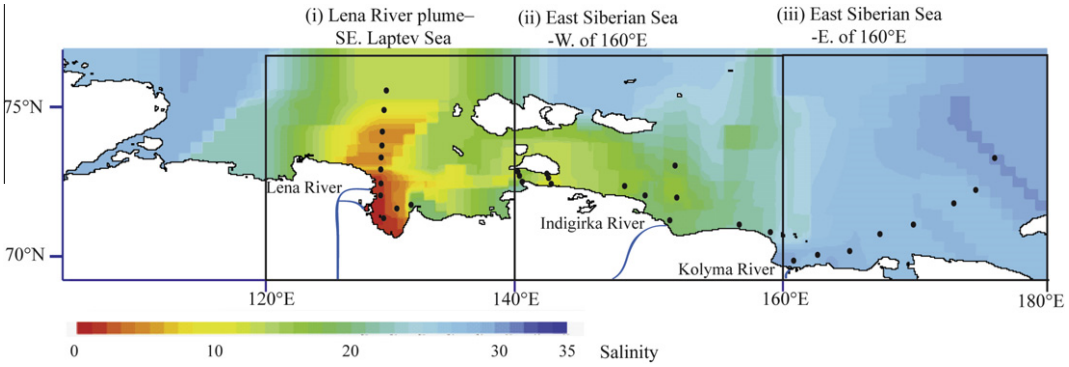

Fig. 1. Sampling points and salinities of the surface waters in the Laptev and East Siberian Seas. Also shown is the division of the ESAS into three regions: the eastern Laptev Sea with the Lena River plume, the East Siberian Sea W. of 160°E, and the East Siberian Sea E. of 160°E.

through the Dmitry Laptev Strait (Semiletov et al., 2005) and into the East Siberian Sea. At ~160°E these waters flow east along with waters from the Indigirka and Kolyma Rivers to meet Pacific inflow waters entering the East Siberian Sea (Anderson et al., 1998; Jakobsson et al., 2004; Semiletov et al., 2005). Throughout the shelf, there is a pronounced halocline at depths of between 8 and 20 m. Freshwater residence times range from less than 2 months within the pronounced Lena River plume and sub-halocline waters in the Laptev Sea (e.g. Alling et al., 2010) to several years in the East Siberian Sea (e.g. Schlosser et al., 1994; Karcher and Oberhuber, 2002; Alling et al., 2010). On the basis of the above hydrographical features, the results are separated here into three regions: The Laptev Sea, the East Siberian Sea W. of 160°E, and the East Siberian Sea E. of 160°E (Fig. 1).

2.2. Measurements of $\delta^{13}C_{DIC}$

For the determination of C isotope compositions in water, we followed similar sampling and preservation techniques to those described in Torres et al. (2005) to minimize the possibility of contamination by CO_2 from air and from biological processes in stored samples. Samples were collected using Niskin bottles attached to a Seabird CTD, and vacuum-filtered onboard with 25 mm diameter precombusted filters (<0.7 mm GF/F filters; Whatman, Inc.) within an all-glass filtration system. After filtration the samples were directly injected with a syringe into 12 ml septum-seal glass vials (Labco Limited), which had been flushed with argon gas (75 mL min^{-1}) for 5 min. Duplicate aliquots (1–4 mL) were taken from each sample. To each vial, 100 µl of 85.5% H_3PO_4 was added to act as a preservative and to transform all the HCO_3^- and CO_3^{2-} ions to $CO_2(g)$. Transfer by needle injection through the septa avoided both air entering the vial and CO_2 leaving it. The samples were stored under cold (+4 °C) and dark conditions until analysis. This method had been tested prior to the sampling cruise and shown to efficiently preserve the samples while avoiding air contamination.

The particulate matter on the GF/F filters were used for POC measurements (Sanchez-Garcia et al., 2011), and the filtrate was also used for DOC measurements (Alling et al., 2010).

The stable carbon isotopic compositions were determined using a Gasbench II extraction line coupled to a Finnigan MAT 252 mass spectrometer. Results are given as per mil deviations from the standard (PDB) and denoted $\delta^{13}C$, where R is the ratio of $^{13}C/^{12}C$:

$$\delta^{13}C(‰) = (R_{sample}/R_{standard} - 1)10^3 \quad (1)$$

From repeated measurements of standards, the reproducibility was calculated to be better than 0.1‰ for $\delta^{13}C$. The sample duplicates showed an even lower variability; sample variation between duplicates was <0.05‰, except for 3 samples, which varied between 0.1‰ and 0.05‰.

For $\delta^{13}C_{POC}$ measurements, the reproducibility was better than ±0.2‰.

2.3. DIC concentrations

The DIC concentrations are from Anderson et al. (2009), with precisions, as determined by duplicate samples, typically of ±1 µmol kg^{-1}. The DIC concentrations used here are either from sample aliquots taken from the same Niskin bottle as those taken for $\delta^{13}C_{DIC}$ measurements, or from a nearby depth from the same cast within the same mixing layer and with similar salinity, as well as with identical DOC concentrations, $\delta^{13}C_{DIC}$ values and temperature. DIC concentration data are available for 70 samples, or approximately 85% of those analyzed for $\delta^{13}C_{DIC}$. The waters of the ESAS are annually impacted by formation, melting, and export of sea ice. These processes in turn effect the DIC concentrations, which could either be diluted by melting of sea ice, or increased due to formation and export of ice. The relative contributions by these processes can be quantified from the measured $\delta^{18}O$ values of each water sample (Östlund and Hut, 1984; Ekwurzel et al., 2001), and the samples are all corrected for such processes. However, salinity variations in the samples of the present study dominantly reflect mixing between river water and seawater (P. Andersson Swedish museum of natural sciences, unpublished data). The correction for this is only significant for the samples from the Laptev Sea below the halocline. Most

samples show just minor influence (<<10%) of the formation and export of sea ice.

3. RESULTS

3.1. $\delta^{13}C_{DIC}$ values and DIC concentrations of ESAS waters

The $\delta^{13}C_{DIC}$ values from the Laptev and East Siberian Sea are shown in Fig. 2A. Data for 83 samples varied between −7.2‰ and 1.6‰, with the isotopically lightest values found close to the Lena River mouth and the heaviest in the surface waters on the outer shelf (Fig. 2A). These data are comparable to the $\delta^{13}C_{DIC}$ values previously found in the Kara and Laptev Seas, which are in the range of −8‰ to 1.45‰ (Erlenkeuser et al., 2003; Bauch et al., 2004). The $\delta^{13}C_{DIC}$ value of the Lena River was estimated to be −8‰ from the low-salinity samples (S < 5) in this dataset. The corresponding data for DIC concentrations are shown in Fig. 2B.

The data can be compared to conservative mixing between Lena River water and Arctic seawater. The DIC concentration in late summer Lena River waters (1997–2010) was 810 ± 79 μM (mean ± 95% confidence interval (CFI 95%), see Fig. 2B), estimated from the PARTNERS dataset for pH, alkalinity and temperature ($n = 5$), which is somewhat higher than the Lena concentration (515 μM) estimated for the late summer seasons (1989 and 1991) by Cauwet and Sidorov (1996). The annual mean concentration of DIC in the Lena River appears to be very similar, based on the flow-weighted annual mean DIC of 822 ± 87 μM from PARTNERS dataset ($n = 20$) (Cooper et al., 2008). Data from other rivers indicate that changes in $\delta^{13}C_{DIC}$ values in river waters are accompanied by changes in DIC concentration (Quay et al., 1992; Dubois et al., 2010). As the August and mean waters seems to have very similar (within 2%) concentrations, the $\delta^{13}C_{DIC}$ values could also be assumed to be very similar in the absence of direct data for the Lena River.

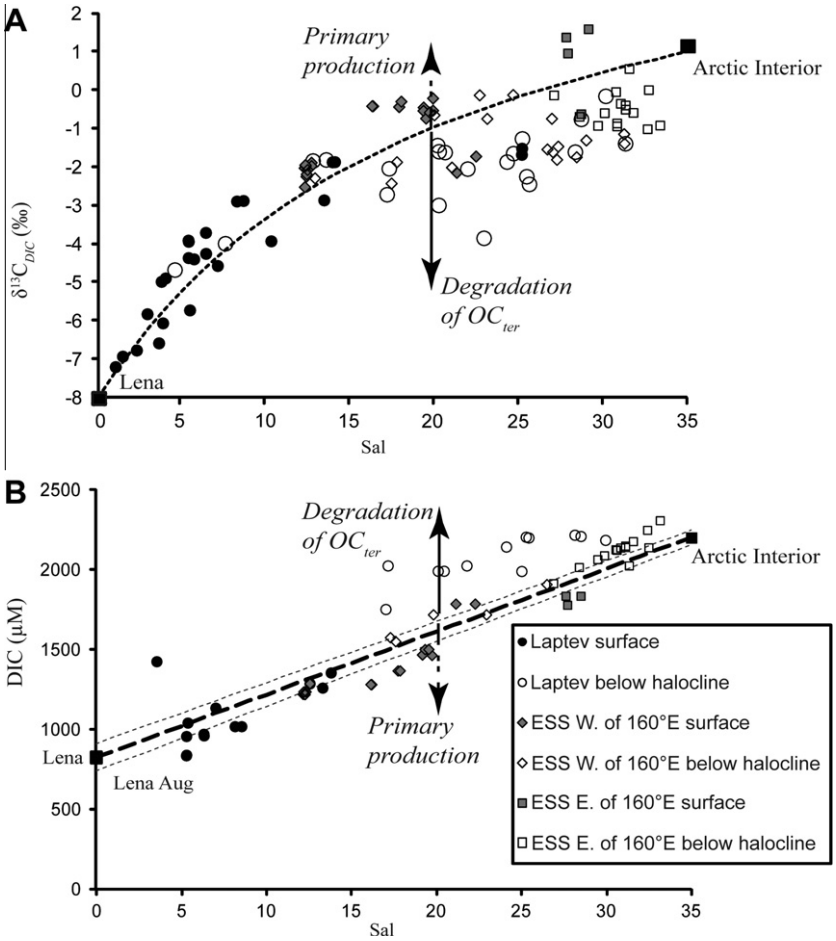

Fig. 2. (A) $\delta^{13}C_{DIC}$ values plotted against salinity, and (B) DIC concentrations plotted against salinity (data from Anderson et al., 2009). Calculated two-component mixing lines are shown. The saline end-member is based upon the composition of waters in the Arctic interior (Anderson et al., 1998; Gruber et al., 1999). The freshwater end-members are the Lena River waters calculated with $\delta^{13}C_{DIC}$ values from this study, and concentrations from the PARTNERS dataset (alk, pH and temp) (Cooper et al., 2008; McClelland et al., 2008). The arrows indicate how degradation of OC_{ter} and carbon fixation during primary production affect the isotope values and concentrations. In (B) the dashed lines represent a 95% confidence interval (CFI) based upon the uncertainty in the calculated flow-weighed mean value for the Lena River waters.

As seen in Fig. 2, many of the samples have compositions of $\delta^{13}C_{DIC}$ and DIC concentrations that do not fall on the line of conservative mixing between Lena River water and Arctic seawater ($\delta^{13}C_{DIC} = 1.45‰$ Gruber et al., 1999; $2200 \pm 2\%$ μM, Anderson et al., 1998). Furthermore, the $\delta^{13}C_{DIC}$ values of the samples show regional variations, as well as strong differences between bottom waters and surface waters. The most pronounced feature in the $\delta^{13}C_{DIC}$ values is that the waters from below the halocline have lighter $\delta^{13}C_{DIC}$ values compared to those expected from conservative mixing. In contrast, some surface waters in the East Siberian Sea exhibit slightly heavier values. The DIC concentrations are generally higher than the conservative mixing line in the waters from below the halocline, and lower in some surface waters from the East Siberian Sea (Fig. 2B).

4. DISCUSSION

4.1. Processes affecting DIC concentrations and $\delta^{13}C$ values

The DIC concentrations and $\delta^{13}C_{DIC}$ signatures vary in the waters of the ESAS due to a number of processes. While mixing between river water and seawater dominates the distribution of DIC concentrations and isotopic compositions, a number of other processes are clearly important as well and may explain deviations from conservative mixing; degradation of OC_{ter}, outgassing of CO_2, and primary production. Approaches for modeling the effects of each of these relevant processes are presented in the next sections, using as a reference the DIC compositions expected from conservative mixing. Both the equations and a graphical method (Fig. 3) for identifying and quantifying the effects of these processes on the DIC concentrations and isotopic compositions are developed. The results will in turn be used to determine to what extent each region is a source or a sink of CO_2 to the atmosphere.

4.1.1. Conservative mixing of DIC concentrations and $\delta^{13}C$ values

The dominant, and most obvious, control on the DIC in the ESAS is the mixing of freshwater and seawater that is evident from the range of salinities. The concentration of DIC in estuarine waters resulting from mixing is

$$[DIC]_R f_R + [DIC]_{SW}(1 - f_R) = [DIC]_{mix} \quad (2)$$

The isotopic composition of DIC resulting from mixing is

$$\delta^{13}C_{mix} = \frac{[DIC]_R \delta^{13}C_R f_R + [DIC]_{SW}\delta^{13}C_{SW}(1 - f_R)}{[DIC]_R f_R + [DIC]_{SW}(1 - f_R)} \quad (3)$$

where [DIC] is the concentration of DIC, the subscript R denotes river water (in this case Lena river water, which dominates the freshwater budget both in the Laptev and the East Siberian Seas), and SW is for sea water (here Arctic Interior water). The subscript mix denotes the mixture of water from conservative mixing of the two end-members. The parameter f_R is the fraction of river water in the mixture and can be calculated from salinities.

In Eq. (3), $\delta^{13}C_{mix}$ is a function only of the salinity of the mixture (represented by f_R), and all the other parameters are defined by the characteristics of the end-members. This equation therefore defines the variations in isotopic composition across a mixing region where there are no other sources or sinks of DIC. Note that $\delta^{13}C_{mix}$ is not a linear function of salinity (Eq. (3) and Fig. 2A).

As seen in the results (Fig. 2) the data cannot be explained only by conservative mixing. Each measured $\delta^{13}C_{DIC}$ value and DIC concentration can be compared to those expected from conservative mixing (Eqs. (2) and (3)), and the deviations from mixing can be defined by the equations (Erlenkeuser et al., 2003)

$$\Delta\delta^{13}C_{DIC} = \delta^{13}C_{sample} - \delta^{13}C_{mix} \quad (4)$$

and

$$\Delta[DIC] = \frac{[DIC]_{sample} - [DIC]_{mix}}{[DIC]_{mix}} \quad (5)$$

$\Delta\delta^{13}C_{DIC}$ represents simply the difference in isotope composition from that expected from conservative mixing ($\delta^{13}C_{mix}$), while Δ[DIC] expresses the deviation in DIC concentration relative to the calculated conservative mixing concentration ($[DIC]_{mix}$). While there is no data of the variation in the $\delta^{13}C_{DIC}$ endmember values, and it could be argued to be minimal (see Section 3.1), there is a natural variance in $[DIC]_R$, which has been estimated from the PARTNERS dataset. This results in an uncertainty in $[DIC]_{mix}$, and so a variance in Δ[DIC]. Mean variance in the Δ[DIC] is ± 0.02. All Δ[DIC] and $\Delta\delta^{13}C_{DIC}$ values are in Table A1 in the Appendix.

The sample values for $\Delta\delta^{13}C_{DIC}$ and Δ[DIC] are plotted in Fig. 3, where the origin represents the values equal to those calculated for conservative mixing of each sample. The samples generally fall in the upper left quadrant of the plot, where elevated $\delta^{13}C_{DIC}$ values ($\Delta\delta^{13}C_{DIC} > 0$) are associated with decreased DIC concentrations ($\Delta[DIC] < 0$), as well as in the lower right quadrant, where depleted $\delta^{13}C_{DIC}$ values ($\Delta\delta^{13}C_{DIC} < 0$) are associated with increased DIC concentrations ($\Delta[DIC] > 0$). There are obvious patterns for the surface waters in the three different areas defined in 2.1 (Fig. 3A). Generally, data for the surface waters of the Laptev and East Siberian Sea W. of 160°E are distributed in the top left quadrant, along with data from the Kara Sea (Erlenkeuser et al., 2003). The similarity between the data from the two areas suggests that the same processes dominate DIC distributions in surface waters of both seas. The surface samples from the East Siberian Sea E. of 160° show no single pattern, but many samples also fall in the upper left quadrant. Other samples have $\Delta\delta^{13}C_{DIC} < 0$ and some even fall in the upper right quadrant. These are the samples closest to the Kolyma River estuary (Table A1). The waters below the halocline (Fig. 3B) generally fall in the region of lower $\delta^{13}C_{DIC}$ values and higher DIC concentrations, even if some samples, especially from the East Siberian Sea W. of 160°E, falls in the upper left quadrant.

The data in Fig. 3 can be explained by the combined effects of four processes: addition of DIC from degradation of OC_{ter} (vectors in the lower right quadrant) and from weathering of $CaCO_3$, (vector in upper right quadrant), and removal of DIC by outgassing of CO_2 (vectors in upper and lower left quadrant) and by carbon fixation in primary

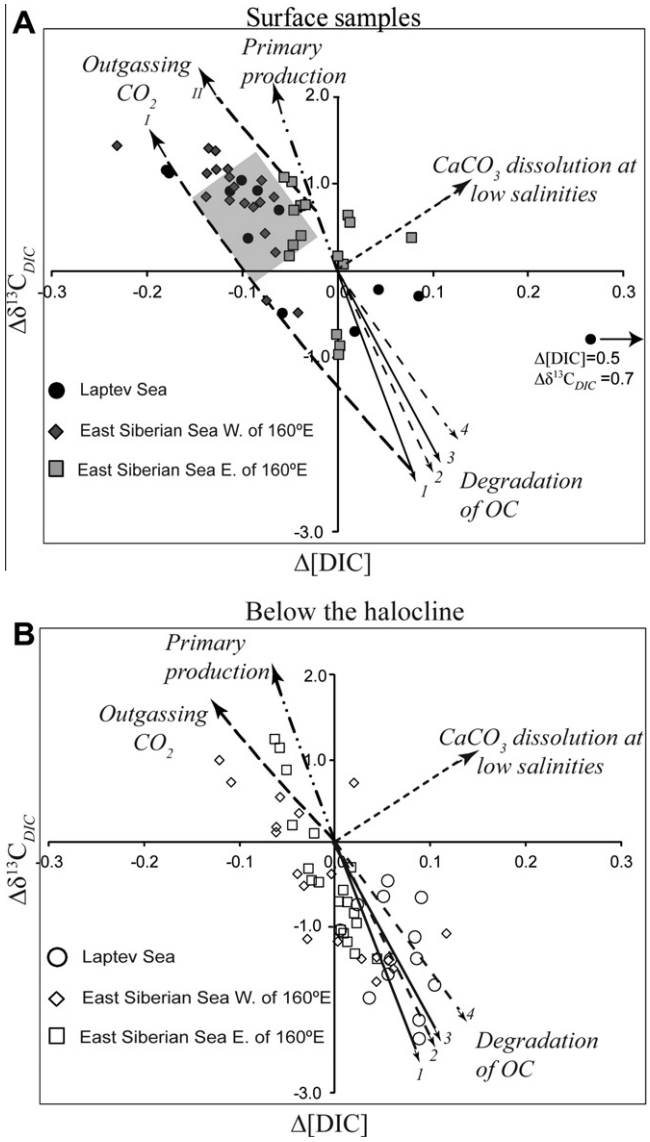

Fig. 3. The changes in $\delta^{13}C_{DIC}$ ($\Delta\delta^{13}C_{DIC}$) and DIC concentrations (Δ[DIC]) relative to those expected from conservative mixing. Also shown are the calculated vectors for the effects of the most likely processes affecting DIC. Four vectors are show for the degradation of OC, as the effect will depend upon the starting DIC composition in the water, and whether the OC is of terrestrial origin ($\delta^{13}C_{OC} = -28‰$, line 1 and 3) or marine ($\delta^{13}C_{OC} = -21‰$, line 2 and 4) and so those for the highest $\delta^{13}C_{mix}$ values (at high salinities; line 1 and 2) and lowest $\delta^{13}C_{mix}$ values (at low salinities; line 3 and 4) are shown. (A) Surface waters. In the Laptev and the East Siberian Sea, most samples have lower [DIC] than expected from conservative mixing, and so fall to the left of the origin. Loss of DIC by primary production alone cannot explain the data except for a few samples in East Siberian Sea E of 160°E; additional loss of DIC with less isotopic fractionation by outgassing of CO_2 is required. Each sample can be explained by a unique net result of addition of DIC from degradation and loss due to primary production, and then loss by outgassing. For example, in the figure two outgassing vectors are shown that bound the area of the samples, starting from greatest and smallest net addition of DIC. The samples require a maximum of 25% outgassing of CO_2 in the Laptev Sea (250 μM) and ~15% (~200 μM) in the western part of East Siberian Sea (compared to $\Delta[DIC]_{mix}$, vector I, concentrations from Table A1). Data for the Kara Sea (Erlenkeuser et al., 2003) falls within the grey box shown. $CaCO_3$ dissolution seems to be important in a few samples from the Laptev Sea close to the Lena River mouth and East Siberian Sea E. of 160°E close to the Kolyma River mouth. (B) Most samples from below the halocline in all three regions fall along the calculated vectors for degradation of OC_{ter} (line 1) or to the left of it, which is consistent with degradation and outgassing. The mean increase in [DIC] is 5%, equal to ~70 ± 20 μM DIC.

production (vector in upper left quadrant). The effects of each process are described in the following sections.

4.1.2. Addition of DIC by degradation of organic carbon

Degradation of OC (both DOC and POC) normally produces DIC without any substantial isotopic fractionation relative to the OC, as shown in experiments by Norrman et al. (1995) and Hullar et al. (1996). Also *in situ* studies of sinking and degradation of particles (Meyers, 1997) found that the isotopic value of the organic carbon substrate did not change even when up to 50% of the material was degraded, and the microbial biomass reflected the iso-

topic composition of the food. Though some studies have shown small effects on the isotopic value of the substrate during degradation (Waite et al., 2005), these effects are small compared to the uncertainties in the value for the organic C degraded (see below). This process will therefore add DIC to the system with a relatively constant $\delta^{13}C_{DIC}$ value. The flow-weighted $\delta^{13}C_{DOC}$ value of the Lena River is −27.0‰ (Raymond et al., 2007). The flow-weighted $\delta^{13}C_{POC}$ value of the Lena River is somewhat lower, −28.4‰, and can periodically be even lower, while the $\delta^{13}C_{DOC}$ value seems to be more stable during the year (PARTNERS dataset, Raymond et al., 2007). Eighty-five percentage of the Lena River OC discharge is DOC, and a large part of both POC and DOC have recently been shown to be removed, possibly by degradation, over the ESAS (Alling et al., 2010; Sanchez-Garcia et al., 2011).

When DIC from degradation of OC_{ter} is added to water with an initial DIC concentration $[DIC]_I$, first established by e.g. mixing between river water and seawater (Section 4.1.1), the concentration is increased by $[DIC]_{OC}$, resulting in a final DIC concentration $[DIC]_{final}$. The fraction of DIC from degraded OC_{ter} is defined as f_{OC}

$$f_{OC} = \frac{[DIC]_{final} - [DIC]_I}{[DIC]_{final}} \quad (6)$$

The resulting isotopic composition of the DIC in the water is

$$\delta^{13}C_{final}[DIC]_{final} = \delta^{13}C_I[DIC]_I + \delta^{13}C_{OC}[DIC]_{OC} \quad (7)$$

Combining with Eq. (6) yields

$$\delta^{13}C_{final} = f_{OC}(\delta^{13}C_{OC} - \delta^{13}C_I) + \delta^{13}C_I \quad (8)$$

This equation provides the isotopic composition for DIC containing some fraction f_{OC} of degraded OC_{ter}. Assuming that the initial composition is equal to that established by conservative mixing before any CO_2 additions, and when Δ[DIC] is considerably less than 1, as with the ESAS samples, f_{OC} and Δ[DIC] are approximately the same. The vectors for degradation of OC_{ter} in Fig. 3 are then defined by

$$\Delta\delta^{13}C \approx \Delta[DIC](\delta^{13}C_{OC} - \delta^{13}C_{mix}) \quad (9)$$

In this case, Δ[DIC] and $\Delta\delta^{13}C_{DIC}$ are linearly related, and the slope of the relationship is negative. As shown in Fig. 3, this can account for samples with relatively large negative $\Delta\delta^{13}C_{DIC}$ values and small positive Δ[DIC] values. For degradation of OC_{ter}, the slope of the line is determined by $\delta^{13}C_{OC} = -27‰$ (PARTNERS dataset and Raymond et al., 2007) and the $\delta^{13}C$ value for conservative mixing for each sample, is between $\delta^{13}C_{mix} = -7‰$ and +1‰. The slope therefore varies between −20 and −28, and those vectors are equal to line 1 and 3 in Fig. 3. Where marine OC is the source of OC, the $\delta^{13}C_{OC}$ value is somewhat higher (up to −21‰); those vectors are equal to line 2 and 4 in Fig. 3A.

Another pool of OC in the ESAS is methane (Shakhova et al., 2010). Degradation of methane has also been considered as a source for DIC on the shelf. While methane is oversaturated in these waters with respect to equilibrium with the atmosphere, the absolute concentrations are still very low- ~100 nM (Shakhova et al., 2010). The [DIC] for the same waters average about 2000 μM, or 2×10^4 times greater. The sampled shelf waters which have the lowest $\delta^{13}C$ values have [DIC] that are ~5% higher than from mixing, i.e. ~100 μM; this is 1×10^3 times greater than the methane concentrations. Assuming that these methane concentrations are representative of the whole year, and that the residence time of water on the shelf is on the order of a year, methane would have to have a residence time of 1×10^{-3} years (~8 h, or a degradation rate of 0.125 h^{-1}) to have produced enough DIC through degradation to be responsible for the changes in the $\delta^{13}C$ values and [DIC]. Reported methane degradation rates are two orders of magnitude slower than that, e.g. 3.8×10^{-3} h^{-1} (Kitidis et al., 2010). Since the methane may have a $\delta^{13}C$ value as low as −40‰, degrading methane at that rate would add 0.1% to [DIC] (Δ[DIC] = 0.001), which would lower a $\delta^{13}C_{DIC}$ value from e.g. 0‰ by only 0.04‰ (Eq. (9)). Consequently, based upon the current knowledge about methane concentrations and degradation rates, the addition of DIC from methane is not considered further in this study.

4.1.3. Loss of DIC through outgassing of CO_2

Degradation of OC_{ter} can lead to an oversaturation of pCO_2 compared to the level for equilibration with the atmosphere, which in turn leads to outgassing of CO_2 from the water and so lowering the [DIC]. It has been shown that surface waters of the Laptev and East Siberian Seas as far as 160°E are oversaturated in pCO_2 (Semiletov et al., 2007; Anderson et al., 2009). This oversaturation could be degradation over the shelf, as well as within the catchment of the river. Often rivers have oversaturated values of pCO_2 (e.g. Humborg et al., 2010), but in the case of the Lena river, less than 10% of the DIC in the river is CO_2, and so the oversaturation in the river is an insignificant addition to the DIC on the shelf. In contrast, the pCO_2 levels in the surface waters of the East Siberian Sea, E. of 160°E, are sometimes undersaturated, which can lead to an uptake of CO_2 from the atmosphere (Pipko et al., 2002; Semiletov et al., 2007; Anderson et al., 2009).

Defining f_{CO_2} as the fraction of DIC in the water remaining after outgassing of CO_2 compared to the initial DIC concentration $[DIC]_I$ before outgassing started, then

$$[DIC]_{final} = f_{CO_2}[DIC]_I \quad (10)$$

outgassing of CO_2 will fractionate the remaining DIC because there is isotopic fractionation between HCO_3^- ions (>90% of total inorganic carbon species in the waters here) and CO_2[aq]. The fractionation factor α between HCO_3^- and CO_2[aq] is temperature dependent and can be estimated using the equation (Rau et al., 1996; and based on Mook et al., 1974)

$$\delta^{13}C_{CO_2} = \delta^{13}C_{DIC} + 23.644 - 9701.5/T \quad (11)$$

where T is the temperature in Kelvin and $\delta^{13}C_{DIC}$ is approximately equal to that of HCO_3^-. The equilibrium fractionation factor ε_{CO_2} is defined as

$$\varepsilon_{CO_2} = \delta^{13}C_{CO_2} - \delta^{13}C_{DIC} \quad (12)$$

The values for ε_{CO_2} for the samples of this study vary between −11.1‰ and −11.9‰ due to temperature differences (Eq. (12)). Using the approximation $\varepsilon \approx 10^3 \ln\alpha \approx 10^3(\alpha - 1)$ (Emerson and Hedges, 2008), then α_{CO_2} values of 0.988–0.989 are obtained for the ESAS. The atmospheric $\delta^{13}C_{CO_2}$ value is −8‰ (Gruber et al., 1999), and so exchange of CO_2 between the waters of the ESAS and the atmosphere will increase the $\delta^{13}C_{DIC}$ values until an equilibrium value of about +3‰ to +4‰ is reached (Eq. (13)). However, this process is >10 times slower than the equilibration of the DIC concentrations (Gruber et al.,1999; Zhang et al., 1995; Lynch-Stieglitz et al., 1995), which has not occurred in these waters (Pipko et al., 2002; Semiletov et al., 2007; Anderson et al., 2009).

When outgassing occurs from oversaturated waters over short time scales, CO_2 transfer can be considered uni-directional; the dominant flux of CO_2 is loss to the atmosphere, and isotopic equilibration by dissolution of atmospheric CO_2 is less significant. The $^{13}C/^{12}C$ ratio (R_{final}) in the remaining waters will be fractionated during progressive outgassing by Rayleigh distillation, and will evolve according to the equation

$$R_{final} = R_I (f_{CO_2})^{\alpha_{CO_2}-1} \quad (13)$$

where R_I is the initial ratio before outgassing started. This equation is equivalent to

$$\delta^{13}C_{final} = \delta^{13}C_I + 10^3(\alpha_{CO_2} - 1)\ln(f_{CO_2}) \quad (14)$$

When only a small amount of DIC has been lost by outgassing, so that $[DIC]_{final}/[DIC]_{mix}$ is close to 1, Eqs. 4, 5, 11, and 15 can be combined to obtain the equation that defines the vector for outgassing in Fig. 3

$$\Delta\delta^{13}C \approx \Delta[DIC](\alpha_{CO_2} - 1)10^3 \quad (15)$$

In this case, since α_{CO_2} ~0.989, there is an almost linear relationship between Δ[DIC] and $\Delta\delta^{13}C_{DIC}$ with a slope of approximately −11. As shown in Fig. 3, outgassing of CO_2 therefore decreases Δ[DIC] and increases $\Delta\delta^{13}C_{DIC}$, and so can at least partly explain the data in the upper left quadrant. In Fig. 3A two outgassing vectors are shown; vector I starts after addition of DIC by degradation of organic C, while vector II starts after net loss of DIC from primary production (see Section 4.3.1).

The extent of CO_2 loss will be determined by a number of factors controlling transfer of CO_2 to the air–water interface, and will depend upon the residence time of water on the shelf. Waters will deviate from this line as equilibrium pCO_2 values are approached and re-equilibration with the atmosphere occurs. This may not occur in the ESAS, where residence times are short. However, exchange with the atmosphere will drive the $\delta^{13}C_{DIC}$ values of oversaturated surface waters in the Laptev and East Siberian Seas towards higher $\delta^{13}C_{DIC}$ values and lower [DIC]. Note that losses can occur from waters that have CO_2 levels above saturation, which is determined by pH and temperature, and which is not readily seen from a simple comparison with the conservative mixing calculations. However, such a comparison (Fig. 3) does identify when outgassing has indeed occurred.

4.1.4. Primary production

Another common process that affects DIC in shelf waters is primary production, which removes carbon through incorporation into organisms. This material then joins the POC pool within the water column or is removed by sedimentation. Primary production incorporates C that is isotopically fractionated compared to DIC, and so progressively changes the DIC isotopic composition. The fractionation factor ε_{PP} is

$$\varepsilon_{PP} = \delta^{13}C_{product} - \delta^{13}C_{substrate} \quad (16)$$

The pathway for carbon fixation in marine phytoplankton is in general not well understood (Roberts et al., 2007 and references therein). Even though CO_2 has been regarded as the main C source for primary production in marine plankton, there is also evidence that some species of phytoplankton use HCO_3^- as a carbon source (e.g. Tortell et al., 1997; Popp et al., 1998), and so there may be a mixture of fractionation mechanisms involved. However, $\delta^{13}C_{POC}$ values of marine-produced POC are well documented and show values of between −19‰ and −23‰ (e.g. Peterson and Fry, 1987). Assuming that marine phytoplankton preferentially use CO_2[aq] as a carbon source with an average $\delta^{13}C_{CO_2}$ value of −8‰, then to reach the observed $\delta^{13}C_{POC}$ value of between −19‰ and −23‰ a fractionation effect of −11‰ to −15‰ is needed. A fractionation close to these values has also been demonstrated in laboratory experiments with marine phytoplankton of 7 different species, including diatoms and dinoflagellates (Burkhardt et al., 1999). Therefore, a value for ε_{PP} of −13‰ between $\delta^{13}C_{CO_2}$ values and $\delta^{13}C_{POC}$ of primary production has been used here.

As noted above, CO_2 is fractionated relative to HCO_3^- (and so DIC) by a fractionation factor that is temperature-dependent (Eq. (12)) and varies between −11.1 and −11.9, so that the combination of the two fractionating processes gives a total fractionation between primary production and DIC of −24 to −25. This assumes that equilibration between CO_2[aq] and HCO_3^- is always faster than losses of CO_2 by primary production, so that the total fractionation of the CO_2 lost relative to DIC is constant for a given temperature. Note that even if other fractionation mechanisms are involved in generating the phytoplankton isotope values, similar values for ε_{PP} to those used for modeling purposes here are still valid based upon direct measurements of phytoplankton.

The final concentration of DIC is related to the initial DIC concentration $[DIC]_I$ by the factor f_{PP}

$$[DIC]_{final} = f_{PP}[DIC]_I \quad (17)$$

Since primary production will progressively change the isotopic composition of the remaining DIC, primary production therefore will change the $\delta^{13}C_{DIC}$ values by Rayleigh distillation (see Fig. 5), so that the resulting final composition of DIC relative to the initial composition as a function of the amount left after primary production (f_{PP}) is

$$\delta^{13}C_{final} = \delta^{13}C_I + 10^3(\alpha_{PP} - 1)\ln(f_{PP}) \quad (18)$$

Table A1
Location, depths and chemical properties of all samples. Included are also the calculated values for conservative mixing between Lena River waters and Arctic Ocean waters, as well as the calculated deviations from conservative mixing for each sample, used in Fig. 3.

							Samples					Calculated conservative mixing		Calculated difference from conservative mixing[a]	
Area	Sample no.	Latitude °N	Longitude °E	Depth m	Salinity[b]	Temp °C	DOC[c] µM	POC[d] µM	$\delta^{13}C_{POC}$[d] ‰	$\delta^{13}C_{DIC}$ ‰	[DIC][b,e] µM	$\delta^{13}C_{DIC}$ ‰	[DIC] µM	$\Delta\delta^{13}C_{DIC}$ ‰	Δ[DIC]
Laptev	4	75.9870	129.9842	4	13.3	5.8	320	7.6	−30.21	−2.86	1260	−2.1	1338 ± 54	−0.48	−0.06 ± −0.06
	11	73.0185	129.9892	3	2.23	11.1	435	53.2	−27.4	−6.77	–	−6.53	898 ± 82	−0.17	–
	11	73.0185	129.9892	4	3.54	10.6	444	57.6	−26.96	−6.58	1425	−5.79	951 ± 79	−0.69	0.50 ± 0.12
	11	73.0185	129.9892	7	17.14	−0.6	328	11.2	−27.51	−2.04	1615	−1.17	1491 ± 45	−1.13	0.08 ± 0.03
	11	73.0185	129.9892	10	21.78	−0.3	240	28.6	−27.19	−2.04	1771	−0.28	1675 ± 33	−1.4	0.06 ± 0.02
	10	73.184	129.9957	3	3.78	10	414	36.2	−27.24	−6.06	1041	−5.66	960 ± 78	−0.29	0.08 ± 0.08
	10	73.184	129.9957	4	5.37	9.6	398	33.8	−26.57	−5.72	1041	−4.88	1023 ± 74	−0.69	0.02 ± 0.07
	10	73.184	129.9957	15	25.27	−0.9	147	26.4	−27.08	−2.24	1972	0.28	1814 ± 24	−2.13	0.09 ± 0.01
	10	73.184	129.9957	20	25.42	−0.9	138	22.7	−27.69	−2.44	1979	0.3	1820 ± 24	−2.35	0.09 ± 0.01
	9	73.3663	129.997	3	8.53	8.1	397	10.8	−30.33	−2.87	1019	−3.59	1149 ± 66	0.92	−0.11 ± 0.05
	9	73.3663	129.997	4	8.15	8.5	289	11.8	−29.91	−2.89	1019	−3.73	1133 ± 67	1.05	−0.10 ± 0.05
	9	73.3663	129.997	15	25.01	−1.2	262	1.7	−28.96	−1.26	1991	0.24	1803 ± 25	−1.71	0.10 ± 0.02
	9	73.3663	129.997	23	28.14	−1.1	161	15.2	−27.13	−1.6	1996	0.67	1927 ± 17	−1.86	0.04 ± 0.01
	7	74.132	129.9997	2	6.32	6.9	432	11.4	−31.35	−4.25	961	−4.46	1061 ± 72	0.38	−0.09 ± 0.06
	7	74.132	129.9997	4	6.31	6.9	425	12.0	−31.04	−3.71	971	−4.47	1061 ± 72	0.93	−0.08 ± 0.06
	7	74.132	129.9997	16	24.11	−1.3	192	6.3	−28.09	−1.86	1865	0.1	1767 ± 27	−1.58	0.06 ± 0.02
	8	73.5657	130.0078	2	5.28	9.5	391	15.1	−31.24	−3.91	836	−4.92	1020 ± 75	1.16	−0.18 ± 0.06
	8	73.5657	130.0078	4	5.29	9.5	451	13.8	−31.4	−3.94	839	−4.92	1020 ± 75	1.13	−0.18 ± 0.06
	8	73.5657	130.0078	14	20.09	−0.8	276	7.2	−28.83	−1.59	1753	−0.58	1608 ± 37	−0.66	0.09 ± 0.02
	8	73.5657	130.0078	14	20.44	−0.8	255	6.3	−28.14	−1.61	1659	−0.51	1692 ± 37	−0.75	0.02 ± 0.02
	6	74.724	130.0163	4	5.29	7.1	440	13.2	−31.75	−4.36	957	−4.92	1020 ± 75	0.71	−0.06 ± 0.06
	6	74.724	130.0163	10	17.02	−1	320	7.2	−28.88	−2.71	1612	−1.2	1486 ± 45	−1.39	0.09 ± 0.03
	6	74.724	130.0163	32	28.49	−1.6	82	6.7	−26.27	−0.75	1951	0.72	1942 ± 16	−1.05	0.01 ± 0.01
	5	75.2658	130.0165	3	7.01	6.5	434	11.9	−31.47	−4.57	1134	−4.17	1088 ± 70	−0.21	0.04 ± 0.06
	5	75.2658	130.0165	30	31.99	−1.6	69	1.5	−28.53	−0.15	2045	1.13	2080 ± 80	−0.65	0.05 ± 0.00
	14	71.6303	130.0495	2	0.98	11.1	442	88.8	−27.13	−7.2	–	−7.32	849 ± 85	0.15	–
	15	71.6282	130.0535	2	1.4	10.7	479	143.3	−26.91	−6.93	–	−7.04	866 ± 84	0.16	–
	15	71.6282	130.0535	4	3.94	8.9	476	25.1	−28.74	−4.89	–	−5.58	966 ± 78	0.81	–
	15	71.6282	130.0535	7	4.48	7.8	471	10.7	−30.19	−4.67	–	−5.31	988 ± 77	0.76	–
	15	71.6282	130.0535	10	22.74	2.8	298	154.2	−26.39	−3.85	–	−0.11	1713 ± 31	−3.36	–
	16	71.627	130.3178	2	2.86	9.8	483	77.7	−27.58	−5.82	–	−6.16	923 ± 81	0.43	–
	16	71.627	130.3178	4	3.69	9	475	37.6	−28.02	−4.98	–	−5.71	957 ± 79	0.84	–
	16	71.627	130.3178	7	7.46	5.2	434	16.6	−29.19	−3.99	–	−3.99	1106 ± 69	0.2	–
	16	71.627	130.3178	11	20.07	0.3	254	101.1	−26.59	−2.99	–	−0.58	1607 ± 37	−2.06	–
	13	71.968	131.7013	3	5.61	7.8	479	10.6	−31.29	−4.39	–	−4.77	1033 ± 74	0.53	–
	13	71.968	131.7013	5	10.17	5.7	454	10.3	−31.07	−3.92	–	−3.02	1214 ± 62	−0.66	–
	13	71.968	131.7013	9	20	−1	150	2.8	−28.73	−1.43	–	−0.59	1604 ± 38	−0.48	–

(*continued on next page*)

Table A1 (*continued*)

							Samples					Calculated conservative mixing		Calculated difference from conservative mixing[a]	
Area	Sample no.	Latitude °N	Longitude °E	Depth m	Salinity[b]	Temp °C	DOC[c] µM	POC[d] µM	$\delta^{13}C_{POC}$[d] ‰	$\delta^{13}C_{DIC}$ ‰	[DIC][b,e] µM	$\delta^{13}C_{DIC}$ ‰	[DIC] µM	$\Delta\delta^{13}C_{DIC}$ ‰	Δ[DIC]
	13	71.968	131.7013	18	24.49	−1	150	50.4	−26.04	−1.64	–	0.16	1783 ± 26	−1.41	–
	12	71.9165	132.5757	3	24.99	−0.3	115	26.9	−27.85	−1.51	–	0.24	1802± 25	−1.36	–
	12	71.9165	132.5757	4	24.98	−0.3	257	18.1	−27.51	−1.67	–	0.23	1802 ± 25	−1.51	–
	12	71.9165	132.5757	12	22.44	−0.8	222	18.7	−27.53	−2.08	–	−0.16	1701 ± 32	−1.54	–
	19	73.0345	133.4562	27	27.58	−1.5	112	6.6	−27.07	−1.38	–	0.6	1905 ± 19	−1.57	–
	20	73.3053	139.8927	2	11.86	6.4	317	14.3	−28.98	−1.86	0	−2.5	1281 ± 58	0.9	
	20	73.3053	139.8927	4	12.45	6.4	315	11.8	−29.22	−1.87	1223	−2.33	1304 ± 57	0.73	−0.06 ± 0.04
	20	73.3053	139.8927	8	12.64	6	305	9	−29.46	−1.83	–	−2.28	1312 ± 56	0.72	–
	20	73.3053	139.8927	8	13.43	6	141	9.3	−29.44	−1.81	1286	−2.06	1343 ± 54	−0.46	0.05 ± 0.04
ESS west	21	73.0892	140.3482	2	11.29	6.6	329	8.9	−29.99	−1.88	1157	−2.67	1266 ± 60	1.04	−0.08 ± 0.04
	21	73.0892	140.3482	4	12.09	6.6	329	9.1	−30.04	−1.97	1240	−2.43	1298 ± 58	0.73	−0.04 ± 0.04
	21	73.0892	140.3482	10	14.91	3.9	300	8.5	−28.34	−1.87	1315	−1.68	1409 ± 50	0.12	−0.06 ± 0.03
	21	73.0892	140.3482	15	23.82	−0.4	164	12.8	−27.53	−1.74	1853	0.06	1760 ± 28	−1.41	0.06 ± 0.02
	22	72.8753	140.6287	2	15.68	2.9	298	20.3	−28.43	−2.14	1325	−1.5	1440 ± 49	−0.34	−0.08 ± 0.03
	22	72.8753	140.6287	4	18.41	1.7	194	13.6	−28.33	−1.72	1476	−0.9	1547 ± 42	−0.48	−0.04 ± 0.03
	22	72.8753	140.6287	16	22.59	0.3	175	16.2	−27.88	−1.61	1605	−0.14	1711 ± 31	−1.09	0.12 ± 0.02
	22	72.8753	140.6287	20	23.14	0.2	174	20.4	−27.59	−1.8	1804	−0.05	1733 ± 30	−1.38	0.04 ± 0.02
	24	73.0482	142.6665	2	10.7	6.3	331	19.5	−28.89	−2.24	1064	−2.85	1243 ± 61	0.86	−0.14 ± 0.04
	24	73.0482	142.6665	4	9.04	6.3	334	16.9	−29.4	−2.18	898	−3.41	1178 ± 65	1.44	−0.23 ± 0.04
	24	73.0482	142.6665	10	11.03	4.8	325	12.7	−28.4	−2.29	1112	−2.75	1256 ± 60	0.71	−0.11 ± 0.04
	24	73.0482	142.6665	15	17.19	2	275	16.2	−27.54	−2.01	1444	−1.16	1499 ± 45	−0.52	−0.03 ± 0.03
	25	73.1432	142.667	2	10.87	6.1	317	9.5	−29.86	−1.97	1100	−2.8	1250 ± 61	1.08	−0.11 ± 0.04
	25	73.1432	142.667	4	11.74	6.1	323	9.5	−29.4	−1.94	1190	−2.54	1284 ± 58	0.85	−0.07 ± 0.04
	25	73.1432	142.667	10	10.87	5.6	317	9.7	−29.4	−2.07	1091	−2.8	1250 ± 61	0.98	−0.12 ± 0.04
	23	72.789	142.6697	2	10.54	6.7	325	14.6	−29.25	−2.02	1060	−2.9	1237 ± 61	1.13	−0.14 ± 0.04
	23	72.789	142.6697	4	11.96	6.6	318	14.4	−29.19	−2.52	1201	−2.47	1293 ± 58	0.22	−0.07 ± 0.04
	23	72.789	142.6697	10	14.66	2.3	315	16.2	−28.04	−2.42	1337	−1.74	1399 ± 51	−0.38	−0.04 ± 0.03
	26	72.4598	150.5957	2	17.54	6.6	192	5.4	−30.06	−0.44	1342	−1.08	1513 ± 44	0.97	−0.11 ± 0.03
	26	72.4598	150.5957	4	18.28	6.6	185	4.8	−29.69	−0.53	1399	−0.93	1542 ± 42	0.74	−0.09 ± 0.02
	26	72.4598	150.5957	10	23.48	−0.5	89	14.4	−29.08	−1.53	1691	0	1746 ± 29	−1.16	−0.03 ± 0.02
	26	72.4598	150.5957	16	24.18	−0.7	61	13.1	−28.26	−1.46	1774	0.11	1774 ± 27	−1.19	0.00 ± 0.02
	30	71.3577	152.1527	2	16.9	5.7	347	15.1	−28.09	−0.73	1313	−1.22	1487 ± 45	0.82	−0.11 ± 0.03
	30	71.3577	152.1527	4	17.82	5.4	198	13.4	−28.3	−0.58	1369	−1.03	1524 ± 43	0.78	−0.10 ± 0.03
	30	71.3577	152.1527	6	17.86	5.2	335	15.4	−27.59	−0.64	1549	−1.02	1525 ± 43	0.71	0.02 ± 0.03
	30	71.3577	152.1527	9	20.17	1.2	164	20.2	−27.11	−0.74	1511	−0.56	1616 ± 37	0.18	−0.06 ± 0.02
	27	72.567	152.3727	2	15.61	5.3	156	5	−30.45	−0.41	1236	−1.51	1437 ± 49	1.41	−0.14 ± 0.03
	27	72.567	152.3727	4	15.75	5.3	169	4.8	−30.35	−0.41	1251	−1.48	1442 ± 48	1.38	−0.13 ± 0.03
	27	72.567	152.3727	14	21.67	−0.8	77	4	−30.31	−0.13	1574	−0.3	1675 ± 33	0.54	−0.06 ± 0.02
	27	72.567	152.3727	18	23.62	−0.8	91	5.2	−28.52	−0.74	1741	0.03	1752 ± 29	−0.38	0.00 ± 0.02
	29	72.1997	153.1657	2	16.63	5.1	151	5.7	−30.11	−0.43	1283	−1.28	1477 ± 46	1.17	−0.13 ± 0.03
	29	72.1997	153.1657	4	17.28	5	91	6.4	−30.4	−0.29	1323	−1.14	1502 ± 44	1.18	-0.12 ± 0.03

	29	72.1997	153.1657	14	22.92	−0.9	129	4	−28.83	−0.12	1655	−0.09	1724 ± 30	0.34	−0.04 ± 0.02
	29	72.1997	153.1657	18	26.84	−0.9	58	7.4	−28.81	−1.3	1927	0.5	1879 ± 20	−1.39	0.03 ± 0.01
	28	72.6508	154.1853	2	19.93	2.3	103	3.5	−30.25	−0.52	1479	−0.61	1607 ± 38	0.44	−0.08 ± 0.02
	28	72.6508	154.1853	4	19.71	2.3	94	4.1	−30.81	−0.21	1463	−0.65	1598 ± 38	0.79	−0.08 ± 0.02
	28	72.6508	154.1853	25	29.11	−0.9	42	5.7	−28.92	−1.14	2085	0.79	1968 ± 15	−1.51	0.06 ± 0.01
	28	72.6508	154.1853	28	28.32	−0.9	47	4.9	−27.86	−1.39	2018	0.7	1937 ± 17	−1.67	0.04 ± 0.01
ESS east	32	70.5665	161.217	3	21.46	4.3	112	16	−28.85	0.334	1582	−0.33	1667 ± 34	1.03	−0.05 ± 0.02
	32	70.5665	161.217	4	21.85	4.3	118	15.4	−29.28	0.124	1612	−0.26	1682 ± 33	0.76	−0.04 ± 0.02
	32	70.5665	161.217	6	24.5	2.1	92	11.5	−28.28	−0.683	1739	0.16	1811 ± 26	−0.46	−0.02 ± 0.01
	32	70.5665	161.217	8	25.12	2	86	16.8	−27.1	−0.617	1776	0.25	1866 ± 25	−0.48	−0.02 ± 0.01
	33	70.1683	161.2173	3	26.52	1.4	121	10.4	−28.29	−0.804	1867	0.46	1866 ± 21	−0.86	0.00 ± 0.01
	33	70.1683	161.2173	4	26.44	1.4	115	10.5	−28.42	−0.915	1861	0.44	1863 ± 21	−0.96	0.00 ± 0.01
	33	70.1683	161.2173	7	27.09	1	132	11.8	−27.92	−0.92	1896	0.53	1889 ± 20	−1.05	0.01 ± 0.01
	31	71.5915	161.6935	2	22.87	2.1	134	5.9	−28.63	0.3	1659	−0.09	1723 ± 30	0.77	−0.03 ± 0.02
	31	71.5915	161.6935	4	22.64	2.1	134	3.9	−29	−0.1	1643	−0.13	1713 ± 31	0.41	−0.04 ± 0.02
	31	71.5915	161.6935	16	24.46	0.7	123	10.8	−28.04	−0.13	1742	0.16	1785 ± 26	0.11	−0.02 ± 0.01
	34	69.7082	162.6887	2	19.44	3.5	88	15.5	−28.28	−0.66	1704	−0.7	1588 ± 39	0.39	0.08 ± 0.03
	34	69.7082	162.6887	4	26.7	0.8	118	16.3	−27.44	−0.65	1868	0.48	1873 ± 21	−0.73	0.00 ± 0.01
	34	69.7082	162.6887	7	27.04	0.8	113	20.2	−27.03	−0.59	1890	0.53	1887 ± 20	−0.71	0.00 ± 0.01
	35	69.817	164.0568	3	26.81	2.7	72	23.4	−27.12	0.17	1885	0.49	1877 ± 21	0.08	0.01 ± 0.01
	35	69.817	164.0568	4	26.35	2.7	78	14	−27.13	0.2	1856	0.43	1859 ± 22	0.18	0.00 ± 0.01
	35	69.817	164.0568	15	28.13	−0.9	65	9.5	−25.83	−0.93	1951	0.67	1929 ± 17	−1.19	0.01 ± 0.01
	35	69.817	164.0568	30	27.9	−0.9	76	17.3	−26.32	−0.86	1934	0.64	1920 ± 18	−1.09	0.01 ± 0.01
	36	69.8165	165.9987	2	27.4	2.4	61	7.1	−26.31	0.81	1918	0.57	1901 ± 19	0.65	0.01 ± 0.01
	36	69.8165	165.9987	4	27.53	2.4	109	6.8	−26.43	0.75	1927	0.59	1906 ± 19	0.56	0.01 ± 0.01
	36	69.8165	165.9987	20	28.16	−1.2	81	5.4	−24.23	−0.04	1960	0.67	1931 ± 17	−0.3	0.02 ± 0.01
	36	69.8165	165.9987	32	27.88	−1.4	91	25.9	−24.39	−0.35	1933	0.64	1920 ± 18	−0.57	0.01 ± 0.01
	37	70.1348	168.0068	4	27.34	2	111	4.4	−26.65	0.34	1799	0.57	1898 ± 19	0.18	−0.05 ± 0.01
	37	70.1348	168.0068	8	26.91	2	102	5	−26.64	0.97	1782	0.51	1882 ± 20	0.86	−0.05 ± 0.01
	37	70.1348	168.0068	31	28.69	−1.3	116	9.6	−25.14	−0.39	1974	0.74	1952 ± 16	−0.72	0.01 ± 0.01
	37	70.1348	168.0068	39	28.9	−1.3	109	15	−24.48	−0.5	1996	0.77	1960 ± 15	−0.85	0.02 ± 0.01
	38	70.6983	169.1315	4	27.99	1.4	73	5.2	−25.28	0.54	1831	0.65	1924 ± 18	0.3	−0.05 ± 0.01
	38	70.6983	169.1315	36	29.19	−1.5	102	7.1	−23.95	-0.58	2013	0.8	1971 ± 15	−0.97	0.02 ± 0.01
	39	71.2192	169.3728	4	28.1	−0.5	46	4.6	−23.49	1.34	1817	0.67	1928 ± 17	1.08	−0.06 ± 0.01
	39	71.2192	169.3728	7	28.1	−0.4	85	5	−23.87	1.38	1813	0.67	1928 ± 17	1.13	−0.06 ± 0.01
	39	71.2192	169.3728	30	28.95	−1.3	93	7.1	−28.43	0.56	1871	0.77	1962 ± 15	0.2	−0.0 ± 0.01
	39	71.2192	169.3728	44	28.67	−1.6	87	12.5	−24.04	−1.01	1989	0.74	1951 ± 16	−1.33	0.02 ± 0.01
	41	71.9682	171.7918	5	28.1	0	64	7.7	−25.61	0.96	1837	0.67	1929 ± 17	0.7	−0.05 ± 0.01
	41	71.9682	171.7918	10	29.01	0	68	7.1	−24.28	1.6	1837	0.78	1964 ± 15	1.23	−0.06 ± 0.01
	41	71.9682	171.7918	32	28.7	−1.6	69	37.1	−21.75	0.01	1895	0.74	1951 ± 16	−0.32	−0.03 ± 0.01
	41	71.9682	171.7918	41	30.01	−1.7	65	20.1	−23.05	−0.91	2089	0.9	2003 ± 13	−1.39	0.04 ± 0.01

[a] Calculated according to Eqs. (4) and (5), and used in Fig. 3.
[b] Corrected for ice effects, quantified from $\delta^{18}O$ measurements.
[c] From Alling et al. (2010).
[d] From Sanchez-Garcia et al. (2011), stdev $\delta^{13}C_{POC} \pm 0.15‰$.
[e] From Anderson et al. (2009).

where $\delta^{13}C_I$ is the initial $\delta^{13}C_{DIC}$ value in the waters, and $\delta^{13}C_{final}$ is the ratio in the remaining water after primary production has reduced the original DIC concentration.

Unlike CO_2 outgassing, this process can continue to remove DIC, with a limit only imposed by biological productivity and not by any re-equilibration process.

The equations for removal of DIC by primary production are analogous to those for removal by outgassing of CO_2 (Eq. (16)). Since $\alpha_{PP} = 0.975$ for removal of CO_2 during primary production, the slope is −25 for removal of small fractions of CO_2. As shown in Fig. 3, primary production decreases Δ[DIC] and increases $\Delta\delta^{13}C_{DIC}$, but has a greater effect on the isotopic composition than CO_2 outgassing, for similar amounts of DIC removal. Note that the line for degradation of OC_{ter} (Eq. (9)) has a similar slope (−20 to −29 depending on salinity), and so based upon the distribution of data in Fig. 3 it is only possible to identify the net effect of loss by primary production and addition by degradation of OC_{ter}, and not to obtain the absolute effect of each of these processes individually.

4.2. Comparison between $\delta^{13}C_{DIC}$ and both $\delta^{13}C_{DOC}$ values and $\delta^{13}C_{POC}$ values

Since C is transferred between DOC, POC and DIC by photosynthesis and degradation, it is informative to contrast the $\delta^{13}C_{DIC}$ data with the $\delta^{13}C_{POC}$ values that are available for the same ISSS-08 samples (Sanchez-Garcia et al., 2011), and with $\delta^{13}C_{DOC}$ values measured in the Lena River and in water leaving the Arctic Ocean (Opsahl et al., 1999; Raymond et al., 2007). A graphical comparison of $\delta^{13}C_{POC}$ and $\delta^{13}C_{DIC}$ values (Fig. 4) suggests that there is no single process that can explain the distribution of the data. For comparison the flow-weighted annual mean $\delta^{13}C_{POC}$ value of −28.2‰ for the Lena River is shown which is obtained using the water discharge values from Cooper et al. (2008), and the $\delta^{13}C_{POC}$ data from the PARTNERS dataset (see McClelland et al., 2008). Even though the Siberian Rivers can show much lower $\delta^{13}C_{POC}$ values during autumn (−29‰ to −36‰), most of the POC is transported during the short spring flood (PARTNERS dataset). The flow-weighted Lena River $\delta^{13}C_{DOC}$ value of −27‰ is from Raymond et al. (2007). The Kolyma River has $\delta^{13}C_{POC}$ values (flow-weighted annual mean of ~−29‰, PARTNERS dataset) that are similar to, or slightly lower than, those of the Lena River. Also, due to both higher water discharge and concentrations, the Lena River annual POC and DOC discharges are approximately 10–15 times bigger than those of the Indigirka and Kolyma combined (Gordeev et al., 1996; Cooper et al., 2008), and most of its discharge flows into the East Siberian Sea (Semiletov et al., 2005). Therefore, the Lena River can be used as the $\delta^{13}C_{POC}$ and $^{13}C_{DOC}$ river endmember for the East Siberian Sea.

Interestingly, the surface samples from the East Siberian Sea west of 160°E that have been shown to have higher $\delta^{13}C_{DIC}$ values compared to those predicted by conservative mixing (Fig. 2), showed low $\delta^{13}C_{POC}$ values of typically −29‰ to −32‰. Such depleted $\delta^{13}C_{POC}$ are unlikely to result from mixing between POC from terrestrial (−28‰) and marine (−21‰) sources. Instead, they are probably caused by primary production, as discussed in detail in Section 4.3.1 (Eqs. 20 and 21). The samples in the outer Lena River plume in the Laptev Sea also had very low $\delta^{13}C_{POC}$ values, although those samples are geographically more restricted and of low salinity waters, and may reflect the low $\delta^{13}C_{POC}$ values of the autumn Lena River waters.

4.3. Surface waters

4.3.1. The Laptev and East Siberian Sea West of 160°E

Waters from this region generally have lower DIC concentrations and higher $\delta^{13}C_{DIC}$ values compared to the val-

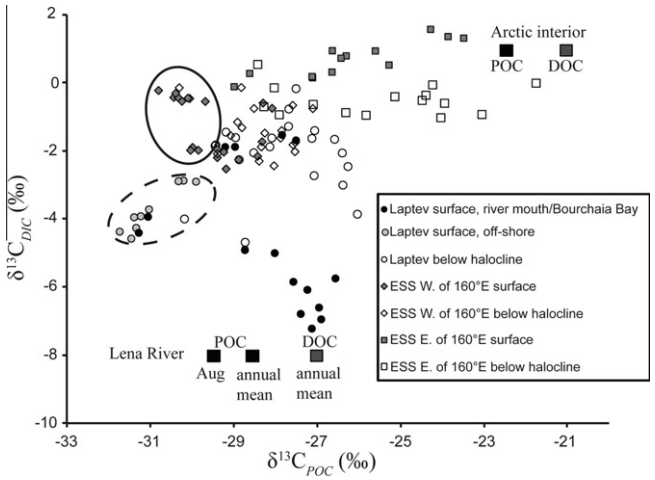

Fig. 4. $\delta^{13}C_{DIC}$ vs $\delta^{13}C_{POC}$ for samples from the ISSS-08 study. The marine (Arctic interior) values are represented by samples from the Fram Strait (Gruber et al., 1999; Stein and Macdonald, 2004) and the riverine values by samples from the Lena River (from the PARTNERS dataset, see McClelland et al., 2008) are shown. Also $\delta^{13}C_{DIC}$ vs $\delta^{13}C_{DOC}$ (instead of $\delta^{13}C_{POC}$) for the endmembers are shown as comparison (Opsahl et al., 1999; Raymond et al., 2007). The samples surrounded by the solid line are those from the East Siberian Sea that had lighter $\delta^{13}C_{POC}$ values than the Lena River, possibly due to uptake of DIC originating from degraded OC_{ter}. The dashed line surrounds other samples from low salinity waters that also had lighter $\delta^{13}C_{POC}$ values than the Lena River, however, these values may be due to temporal changes in the river component.

ues expected from conservative mixing (Fig. 3). Loss of DIC by primary production alone cannot explain the data. Samples that fall to the left of the combined vector for primary production and degradation of OC_{ter} in Fig. 3 also require outgassing of CO_2 (Eq. (16)). The magnitude of the outgassing, and net addition of DIC from degraded OC_{ter} (f_{CO_2} and f_{OC}), can then be estimated by considering two separate steps: (i) net addition of DIC (the net effect of degradation plus primary production) to produce an intermediate DIC concentration and $\delta^{13}C_{DIC}$ value (see Eq. (8)), and (ii) losses of DIC by Rayleigh distillation during outgassing of CO_2 (see Eq. (15)). The magnitude of these processes can be estimated graphically by using the vectors in Fig. 3. Note that loss by primary production and addition by OC degradation are in opposite directions, and so together define a range on approximately a single vector of net loss or gain of DIC by these two processes. The two outgassing vectors shown enclose almost all of the data in the upper left quadrant, and so define the range of net loss or gain of C from primary production plus OC degradation that is required to explain the data. Note that the net addition of DIC from degraded OC_{ter} is a minimum estimate of the total amount of OC degradation, as there may have been greater additions that were offset by losses by primary production. Where f_{OC} is negative, removal by primary production was greater than addition by organic carbon degradation. Fig. 3 demonstrates that each composition to the left of the line for primary production and degradation of organic carbon can be explained by a unique combination of net DIC addition by degradation of OC_{ter} and losses of CO_2.

There are a few exceptions from this pattern in the Laptev Sea surface waters, where the samples show higher [DIC] and lower $\delta^{13}C_{DIC}$ values that expected from conservative mixing. Those values could be explained by a combination of additions from OC_{ter} and another source of C with heavier $\delta^{13}C$ values. This source could be $CaCO_3$, with a $\delta^{13}C_{CaCO3}$ value of 0‰, which at these salinities would result in the vector for $CaCO_3$ dissolution shown in Fig. 3 (derivation of this vector is equivalent to the derivation for additions from OC_{ter}, Eq. (9)).

These samples, unlike those from elsewhere (Laptev Sea further out on the shelf and East Siberian Sea) have very low salinities and so are most sensitive to the DIC concentration of the river water (Fig. 2B). Note that the resulting Δ[DIC] values of 0.04–0.5 correspond to additions of 46–475 μM of DIC; the large relative shift in [DIC] correspond to low absolute additions, because these low salinity samples have low [DIC]. Therefore, the magnitude of the contribution from $CaCO_3$ is uncertain.

The pCO_2 levels in the Laptev and East Siberian Sea west of 160°E were oversaturated compared to those for equilibration with the atmosphere (Anderson et al., 2009) and the samples from this area have DIC concentrations as low as 23% lower than $[DIC]_{mix}$. Combining these concentrations with the $\delta^{13}C_{DIC}$ values (Fig. 3), it is clear that the samples require net additions from degradation of OC_{ter}, equal to 0–10 ± 2% of $[DIC]_{mix}$ (see also Table A1). Therefore, total losses to the atmosphere of 0–15% of $[DIC]_{mix}$, with a mean value of 8 ± 2%, are required (Fig. 3). Excluding the three samples with very high [DIC] and possible additions from $CaCO_3$, the mean calculated loss of CO_2 is then equivalent to 80 ± 60 μM in the Laptev Sea and 140 ± 50 in the East Siberian Sea W. of 160°E, and so this area (120–160°E) is clearly a source of CO_2 to the atmosphere during the ice-free season.

Some of the DIC added from degraded OC_{ter} might have been used by primary production and not outgassed as CO_2, and this can be seen in the $\delta^{13}C_{POC}$ values from the East Siberian Sea W. of 160°E (Fig. 4). While low $\delta^{13}C_{POC}$ values in the Arctic Ocean usually have simply been equated with the composition of the terrestrial input (Stein and MacDonald 2004), this is not consistent to the $\delta^{13}C_{POC}$ values and $\delta^{13}C_{DIC}$ values here. The very light $\delta^{13}C_{POC}$ values could be caused by phytoplankton that have used DIC that has $\delta^{13}C_{DIC}$ values found in this study, and that partly originates from riverine DIC and degraded OC_{ter}, rather than only reflect differences in the terrestrial $\delta^{13}C_{POC}$ values. Unusually low $\delta^{13}C_{POC}$ values in plankton caused by isotopically light DIC are reported from limnic waters (Peterson and Fry, 1987) and from temperate estuaries (Coffin et al., 1994; Chanton and Lewis, 2002; Ahad et al., 2008), but the low $\delta^{13}C_{POC}$ values often found in samples from the Arctic Ocean have not been clearly connected to the DIC system.

The integrated isotopic composition of the produced plankton as the DIC composition evolves, i.e. the accumulated $\delta^{13}C_{POCacc}$ value, can be derived from

$$f_{PP}\delta^{13}C_{final} + (1 - f_{PP})\delta^{13}C_{POCacc} = \delta^{13}C_I \quad (19)$$

where f_{PP} is the fraction of DIC remaining in the water, and $\delta^{13}C_{final}$ and $\delta^{13}C_I$ are the final and initial $\delta^{13}C$ values of DIC, respectively.

The variable $\delta^{13}C_{final}$ can be eliminated by combining Eqs. 1, 14, and 20, and solving for $\delta^{13}C_{POCacc}$

$$\delta^{13}C_{POCacc} = \left(\frac{(f_P P)^{\alpha_{PP}} - 1}{(f_{PP}) - 1}\right)(\delta^{13}C_I + 10^3) - 10^3 \quad (20)$$

The changes due to Rayleigh distillation from removal of C by primary production on the remaining DIC $\delta^{13}C$ values (Eq. (19)), the instantaneously produced $\delta^{13}C_{POC}$ values (Eqs. (13) and (17)), and the accumulated POC production values ($\delta^{13}C_{POCacc.}$, Eq. (20)) are shown graphically in Fig. 5. How $\delta^{13}C_{POC}$ values of −21‰ are generated in full marine waters (S = 35) is shown in Fig. 5A. This is compared with the situation in typical ESAS waters with a salinity of 15, and with additions of DIC from degradation of OC_{ter}. The lighter DIC $\delta^{13}C_{mix}$ values and the added DIC from OC_{ter} (f_{OC}) in the ESAS waters shift the fractionation lines in the vertical direction, creating lighter $\delta^{13}C_{POCacc}$ than usually found in marine environments.

The calculated $\delta^{13}C_{POCacc}$ values can then be compared to the measured $\delta^{13}C_{POC}$ values (Sanchez-Garcia et al., 2011). If the initial $\delta^{13}C_{DIC}$ value is due only to conservative mixing (−1.4‰ in the East Siberian Sea W. of 160°E, Table A1), then the mean initial value for $\delta^{13}C_{POC}$ (from primary production) in this region is −26‰ (Eq. (17), conservative mixing values for DIC from Table A1), and progressively increases as more of the DIC is used for primary production (Fig. 5). Winter NO_3^- concentrations in the region are on the order of 10 μM, and assuming a

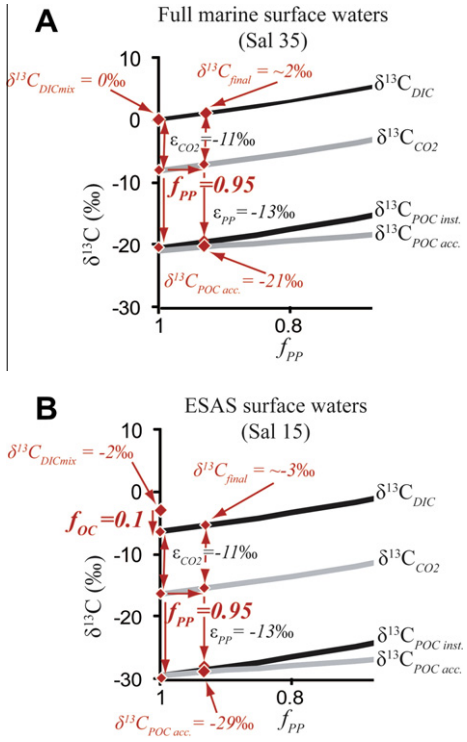

Fig. 5. Fractionation of DIC and POC through Rayleigh distillation in waters that lose DIC through the process of C fixation in marine phytoplankton (f_{PP} = fraction DIC left in the waters). The isotopic fractionation effect ε between HCO_3 (~DIC) and CO_2 is −11‰ to −12‰, and −13‰ between the CO_2 in the water and the C in the instantaneously produced POC is ($\delta^{13}C_{CO_2} - \delta^{13}C_{POCinst}$). Panel A shows this fractionation process for full marine surface waters, generating the widely adopted $\delta^{13}C_{POCacc}$ value of −21‰. Panel B shows the same process for ESAS surface waters, here with a salinity of 15. The already low initial $\delta^{13}C_{DICmix}$ value of −2‰ is further lowered by 2.8–10% addition by degradation of OC. This gives unusually low $\delta^{13}C_{POCacc}$ values, here −29‰, which could explain the very low $\delta^{13}C_{POC}$ values found in bulk POC in the surface waters of the ESAS (Sanchez-Garcia et al., 2011).

Redfield ratio of C/N = 7, some 70 μM POC can be produced, which would lower the DIC concentration by less than 5% (Anderson et al., 2009). If only 5% of the total DIC was used ($f_{PP} = 0.95$), then the calculated $\delta^{13}C_{POCacc}$ values for the surface samples in the western East Siberian Sea are close to −26‰ (Fig. 5). However, the average $\delta^{13}C_{POC}$ measured in those samples are substantially lower (−30‰, Sanchez-Garcia et al., 2011). This can be explained if the $\delta^{13}C_{DIC}$ value is 4‰ lower (i.e. −5.4‰), which can be achieved by a ~12% addition of DIC from degradation of OC_{ter} (Eqs. (8) and (9), see also Fig. 5). However, the measured $\delta^{13}C_{DIC}$ values are higher than −5.4‰, as they reflect not only the addition of DIC from degraded OC_{ter}, but also losses of DIC by outgassing of CO_2 and primary production as described above (illustrated by Fig. 3). The POC therefore appears to have been produced prior to outgassing. Alternatively, the POC seen here may have been produced in waters of lower salinity and therefore lower values of $\delta^{13}C_{DIC}$ (see Figs. 2 and 4). Overall, although the POC has a very low $\delta^{13}C$ value, it can be derived from marine production.

The alternative explanation for the very low $\delta^{13}C_{POC}$ values is that the POC is composed primarily of terrestrial OC. However, the flow-weighed Lena $\delta^{13}C_{POC}$ value of ~−28‰, (PARTNERS dataset) is not sufficiently low. If there is any such terrestrial C included in the POC, then the marine component must be even lower than −30‰ in order to result in a bulk value of −30; this in turn would require that the isotopic composition of the DIC from which the marine component is derived is correspondingly lower than −5.4‰ due to a greater proportion of degraded OC_{ter}.

Therefore, if primary production is assumed to use up 5% of the DIC ($f_{PP} = 0.05$) the measured $\delta^{13}C_{DIC}$ values in the East Siberian Sea W. of 160°E could be the result of a combination of ~10% addition of degraded OC_{ter}, ~5% removal of DIC from primary production (resulting in a net DIC addition from OC_{ter} degradation of 5%) and ~10% DIC outgassed to the atmosphere (as inferred from mean values, Table A1). This could be described in Fig. 3 by moving down on the vector for degradation of OC_{ter} to Δ[DIC] = 0.1, moving up along the primary production vector (which has approximately the same slope as the degradation vector) to a Δ[DIC] value of 0.05, and then moving along the outgassing vector to the left, landing on a Δ[DIC] value of −0.05. Therefore, the pattern seen in Fig. 3 supports an addition of 10% of DIC from degradation of OC_{ter}, so that the very low $\delta^{13}C_{POC}$ values seen in this region reflect marine values that are produced as a consequence of the processes affecting the DIC system seen in this study. An important implication of this is that any mixing models for identifying the proportion of terrestrial C in POC in the Arctic Ocean must consider the possibility of unusually low $\delta^{13}C_{POC}$ in the marine fraction.

4.3.2. The East Siberian Sea East of 160°E

The pCO_2 values for samples collected in the summer from the East Siberian Sea, east of 160 °E, have been reported to be undersaturated with respect to equilibration with the atmosphere (Pipko et al., 2002; Semiletov et al., 2007; Anderson et al., 2009). However, the $\delta^{13}C_{DIC}$ values, combined with the DIC concentrations (Fig. 3), showed somewhat surprisingly that in about half of those samples, outgassing of CO_2 also seemed to have occurred. Degradation of OC_{ter} occurs all year round and during the long winter DIC concentrations increase under the ice (Striegl et al., 2001; Algesten et al., 2006). When the ice cover disappears, the excess DIC can outgas, and simultaneously phytoplankton start to grow and decrease the DIC concentrations. At the end of the ice-free season, when the sampling took place and NO_3^- concentrations in the surface layer were depleted, the primary production had used enough CO_2 to drive the pCO_2 to undersaturated levels, but the $\delta^{13}C_{DIC}$ values still carry the memory of the outgassing event earlier in the ice-free season. These waters were likely to have been outgassed in this region rather than further west and then transported here, as the boundary to eastwards flowing coastal currents is at ~160°E (Semiletov et al., 2005). The East Siberian Sea east of 160°E therefore seems to act as a source of CO_2 to the atmosphere during parts of the year, but as a sink during at least the end of the Siberian summer.

Comparing the patterns in Figs. 3 and 4 for the surface samples in this region, it is clear that primary production is important for many of the samples, since the samples that fall on the vector for primary production in Fig. 3 with high (>0‰) $\delta^{13}C_{DIC}$ values (Fig. 4) also have high (>−27‰) $\delta^{13}C_{POC}$ values. Measured $\delta^{13}C_{POC}$ values of −24‰ for the mid- to outer shelf, is consistent with primary production generated from DIC that has resulted only from conservative mixing. The samples closer to land have POC values between −25‰ and −29‰ (Fig. 4) that might reflect terrestrial POC originating from the Kolyma River, which has a measured values of −29‰ (PARTNERS dataset) and coastal erosion (Vonk et al., 2010; Sanchez-Garcia et al., 2011).

4.4. Bottom waters

Most samples from below the halocline in all three areas fall along, or to the left of, the calculated vectors for degradation of OC_{ter}, indicating that some [DIC] has been outgassed, either during times of turnover, or by bubbles penetrating the halocline. The relative additions of DIC originating from degraded OC_{ter} is highest in the Laptev Sea, reaching as high as 20% of the concentrations expected from conservative mixing, to 5% in the eastern East Siberian Sea.

The approximate mean f_{OC} in the bottom waters, as calculated in Eq. (8) is 0.05, which corresponds to an addition of 5% of the DIC originating from degraded OC_{ter} compared to $[DIC]_{mix}$, which translates to roughly 70 ± 20 μM addition in the waters below the halocline in the ESAS (Eq. (6), $[DIC]_{mix}$ mean value of 1400 μM, Table A1).

OC_{ter} degradation could involve both DOC_{ter} and POC_{ter}. While earlier studies had assumed that DOC_{ter} does not degrade over the shelves in the Arctic (i.e. Köhler et al., 2003; Amon, 2004), this has been challenged in more recent studies (i.e. Cooper et al., 2005; Alling et al., 2010; Letscher et al., 2011), and for the ESAS, DOC_{ter} removal in the bottom waters has been estimated to be 90 μM (Alling et al., 2010). The degradation of POC_{ter} has been estimated as approximately half of that value (Sanchez-Garcia et al., 2011). These numbers agree well with the 70 ± 20 μM found in this study, considering that all three estimates are very approximate. This supports the conclusions that DOC_{ter}, as well as POC_{ter}, degrades during transport over the Arctic shelves, and that DOC_{ter} degradation is responsible for a major part of the DIC increase and so the CO_2 flux to the atmosphere, as suggested by a number of recent studies (Cooper et al., 2005; van Dongen et al., 2008; Anderson et al., 2009; Manizza et al., 2009; Alling et al., 2010; Vonk et al., 2010; Letscher et al., 2011; Sanchez-Garcia et al., 2011).

5. CONCLUSIONS

The results of this study demonstrate that the DIC system in the ESAS is affected by at least four different processes adding and removing DIC. These processes are inferred from the deviations in $\delta^{13}C_{DIC}$ values and [DIC] relative to the values predicted by conservative mixing of Lena River waters and Arctic Ocean waters. Most importantly, the study shows that the DIC concentrations have increased due to degradation of OC_{ter} across the shelf. The average addition of DIC is equal to 70 ± 20 μM, which is consistent with earlier estimates of both DOC_{ter} and POC_{ter} degradation.

In the surface waters of the Laptev and the East Siberian Sea, west of 160°E, the $\delta^{13}C_{DIC}$ values and DIC concentrations indicate that degradation of OC_{ter} has resulted in outgassing of CO_2 to the atmosphere, consistent with earlier studies that have shown that pCO_2 is oversaturated relative to equilibrium with the atmosphere (Anderson et al., 2009). Bottom waters from the ESS w. of 160°E, but not from the Laptev Sea also show significant losses due to outgassing. Surprisingly, although the East Siberian Sea east of 160°E has been shown to be a sink for CO_2 during sampling at the end of the ice-free season (Pipko et al., 2002; Anderson et al., 2009), the combined data for $\delta^{13}C_{DIC}$ values and concentrations indicate that this region has actually acted as a source at other times during the ice-free season. At a few locations, additions of DIC from weathering of $CaCO_3$ have also been identified.

A comparison between the results for the DIC system and data for POC (Sanchez-Garcia et al., 2011) indicates that the low $\delta^{13}C_{POC}$ values seen in this region can be explained by the processes affecting the DIC system. An important implication of this is that any mixing models for describing the cycling of terrestrial POC in the Arctic must consider the possibility of an unusually low $\delta^{13}C_{POC}$ marine end-member.

Understanding the carbon system on the Arctic shelves is essential for understanding global C fluxes and the cycling between OC_{ter} and atmospheric CO_2, and ultimately for understanding the feedbacks in the global climate system. This study shows that isotopic measurements of DIC in shelf waters can provide valuable information for constraining these processes. The modeling approach presented in this paper provides a tool for determining the magnitude of each of these processes for any areas from just the measurements of DIC concentrations and $\delta^{13}C_{DIC}$.

ACKNOWLEDGEMENTS

The ISSS-08 program was supported by the Knut and Alice Foundation, the Far Eastern Branch of the Russian Academy of Sciences, the Swedish Research Council (VR Contract No. 211 621-2007-4631), the US National Oceanic and Atmospheric Administration, the Russian Foundation of Basic Research, the Swedish Polar Research Secretariat, and the Stockholm University Bert Bolin Centre for Climate Research. We thank Igor Semiletov, the crew of the R/V Smirinsky, and the other scientists participating in the ISSS-08 cruise who have provided help and support for this project. We also thank Heike Siegmund for her work in developing the analytical methods for $\delta^{13}C_{DIC}$ and for analyzing the $\delta^{13}C$.

REFERENCES

Ahad J. M. E., Barth J. A. C., Ganeshram R. S., Spencer R. G. M. and Uher G. (2008) Controls on carbon cycling in two

contrasting temperate zone estuaries: the Tyne and Tweed, UK. *Estuar. Coast. Shelf Sci.* **78**, 685–693.

Algesten G., Brydsten L., Jonsson P., Kortelainen P., Lofgren S., Rahm L., Raike A., Sobek S., Tranvik L., Wikner J. and Jansson M. (2006) Organic carbon budget for the Gulf of Bothnia. *J. Mar. Syst.* **63**, 155–161.

Alling V., Sanchez-Garcia L., Porcelli D., Pugach S., Vonk J. E., van Dongen B., Morth C. M., Anderson L. G., Sokolov A., Andersson P., Humborg C., Semiletov I. and Gustafsson O. (2010) Nonconservative behavior of dissolved organic carbon across the Laptev and East Siberian seas. *Global Biogeochem. Cycles* **24**, GB4033. http://dx.doi.org/10.1029/2010GB003834.

Amon R. M. W. (2004) The role of dissolved organic matter for the organic caron cycle in the Arctic Ocean. In *The Organic Carbon Cycle in the Arctic Ocean* (eds. R. Stein and R. W. Macdonald). Springer, pp. 83–99.

Anderson L. G., Jutterstrom S., Hjalmarsson S., Wahlstrom I. and Semiletov I. P. (2009) Out-gassing of CO_2 from Siberian Shelf seas by terrestrial organic matter decomposition. *Geophys. Res. Lett.* **36**, L20601.

Anderson L. G., Olsson K. and Chierici M. (1998) A carbon budget for the Arctic Ocean. *Global Biogeochem. Cycles* **12**, 455–465.

Bauch H. A., Erlenkeuser H., Bauch D., Mueller-Lupp T. and Taldenkova E. (2004) Stable oxygen and carbon isotopes in modem benthic foraminifera from the Laptev Sea shelf: implications for reconstructing proglacial and profluvial environments in the Arctic. *Mar. Micropaleontol.* **51**, 285–300.

Burkhardt S., Riebesell U. and Zondervan I. (1999) Effects of growth rate, CO_2 concentration, and cell size on the stable carbon isotope fractionation in marine phytoplankton. *Geochim. Cosmochim. Acta* **63**, 3729–3741.

Cauwet G. and Sidorov I. (1996) The biogeochemistry of Lena River: organic carbon and nutrients distribution. *Mar. Chem.* **53**, 211–227.

Chanton J. and Lewis F. G. (2002) Examination of coupling between primary and secondary production in a river-dominated estuary: Apalachicola Bay, Florida, USA. *Limnol. Oceanogr.* **47**, 683–697.

Coffin R. B., Cifuentes L. and Elderidge P. M. (1994) The use of stable carbon isotopes to study microbial processes in esturaies. In *Stable Isotopes in Ecology and Environmental Science* (eds. K. Lajtha and R. Michener). Blackwell Scientific Publication, Oxford, UK, pp. 222–241.

Cooper L. W., Benner R., McClelland J. W., Peterson B. J., Holmes R. M., Raymond P. A., Hansell D. A., Grebmeier J. M. and Codispoti L. A. (2005) Linkages among runoff, dissolved organic carbon, and the stable oxygen isotope composition of seawater and other water mass indicators in the Arctic Ocean. *J. Geophys. Res. Biogeosci.* **110**, G02013.

Cooper L. W., McClelland J. W., Holmes R. M., Raymond P. A., Gibson J. J., Guay C. K. and Peterson B. J. (2008) Flow-weighted values of runoff tracers (delta 18O, DOC, Ba, alkalinity) from the six largest Arctic rivers. *Geophys. Res. Lett.* **35**, L18606.

Dittmar T. and Kattner G. (2003) The biogeochemistry of the river and shelf ecosystem of the Arctic Ocean: a review. *Mar. Chem.* **83**, 103–120.

Dubois, K. D., Lee, D. and Veizer, J. (2010). Isotopic constraints on alkalinity, dissolved organic carbon, and atmospheric carbon dioxide fluxes in the Mississippi River. *J. Geophys. Res. Biogeosci.* **115**, http://dx.doi.org/10.1029/2009JG001102.

Ekwurzel B., Schlosser P., Mortlock R. A., Fairbanks R. G. and Swift J. H. (2001) River runoff, sea ice meltwater, and Pacific water distribution and mean residence times in the Arctic Ocean. *J. Geophys. Res. Oceans* **106**, 9075–9092.

Emerson S. R. and Hedges J. I. (2008). , p. 464.

Erlenkeuser H., Cordt H. H., Simstich J., Bauch D. and Spielhagen R. F. (2003) DIC stable carbon isotope pattern in the surface waters of the southern Kara Sea, September 2000. In *Siberian River Run-off in the Kara Sea* (eds. R. Stein, K. Fahl, D. K. Fütterer, E. M. Galimov and O. V. Stepanets), pp. 281–307. Chemical Oceanography and the Marine Carbon Cycle. Elsevier Science, Amsterdam.

Frey K. E. and McClelland J. W. (2009) Impacts of permafrost degradation on arctic river biogeochemistry. *Hydrol. Process.* **23**, 169–182.

Gordeev V. V., Martin J. M., Sidorov I. S. and Sidorova M. V. (1996) A reassessment of the Eurasian river input of water, sediment, major elements, and nutrients to the Arctic Ocean. *Am. J. Sci.* **296**, 664–691.

Gruber N., Keeling C. D., Bacastow R. B., Guenther P. R., Lueker T. J., Wahlen M., Meijer H. A. J., Mook W. G. and Stocker T. F. (1999) Spatiotemporal patterns of carbon-13 in the global surface oceans and the oceanic Suess effect. *Global Biogeochem. Cycles* **13**, 307–335.

Guo L. and Macdonald R. W. (2006) Source and transport of terrigenous organic matter in the upper Yukon River: evidence from isotope (delta C-13, Delta C-14, and delta N-15) composition of dissolved, colloidal, and particulate phases. *Global Biogeochem. Cycles* **20**, GB2011.

Hullar M., Fry B., Peterson B. and Wright R. (1996) Microbial utilization of estuarine dissolved organic carbon: a stable isotope tracer approach tested by mass balance. *Appl. Environ. Microbiol.* **62**, 2489–2493.

Humborg C., Morth C., Sundbom M., Borg H., Blenckner T., Giesler R. and Ittekkot V. (2010) CO_2 supersaturation along the aquatic conduit in Swedish watersheds as constrained by terrestrial respiration, aquatic respiration and weathering. *Global Change Biol.* **16**, 1966–1978.

Jakobsson M., Grantz A., Kristoffersen Y. and Macnab R. (2004) The Arctic Ocean: boundary conditions and background information. In *The Organic Carbon Cycle in the Arctic Ocean* (eds. R. Stein and G. M. MacDonald). Springer Verlag, Berlin Heidelberg, pp. 1–6.

Jakobsson M., Macnab R., Mayer L., Anderson R., Edwards M., Hatzky J., Schenke H. W. and Johnson P. (2008) An improved bathymetric portrayal of the Arctic Ocean: implications for ocean modeling and geological, geophysical and oceanographic analyses. *Geophys. Res. Lett.* **35**, L07602.

Karcher M. J. and Oberhuber J. M. (2002) Pathways and modification of the upper and intermediate waters of the Arctic Ocean. *J. Geophys. Res. Oceans* **107**, 3049.

Kitidis V., Upstill-Goddard R. C. and Anderson L. G. (2010) Methane and nitrous oxide in surface water along the North-West Passage, Arctic Ocean. *Mar. Chem.* **121**, 80–86.

Köhler H., Meon B., Gordeev V. V., Spitzy A. and Amon R. M. W. (2003) Dissolved organic matter (DOM) in the estuaries of Ob and Yenisei and the adjacent Kara Sea, Russia. In *Siberian River Run-off in the Kara Sea* (eds. R. Stein, K. Fahl, D. K. Fütterer, E. M. Galimov and O. V. Stepanets). Elsevier, pp. 281–307.

Letscher R. T., Hansell D. A. and Kadko D. (2011) Rapid removal of terrigenous dissolved organic carbon over the Eurasian shelves of the Arctic Ocean. *Mar. Chem.* **123**, 78–87.

Lynch-Stieglitz J., Stocker T. F., Broecker W. S. and Fairbanks R. G. (1995) The influence of air-sea exchange on the isotopic composition of oceanic carbon – observations and modeling. *Global Biogeochem. Cycles* **9**, 653–665.

Manizza M., Follows M. J., Dutkiewicz S., McClelland J. W., Menemenlis D., Hill C. N., Townsend-Small A. and Peterson B. J. (2009) Modeling transport and fate of riverine dissolved

organic carbon in the Arctic Ocean. *Global Biogeochem. Cycles* **23**, GB4006.

McClelland J. W. and Holmes R. M., et al. (2008) Development of a pan-arctic database for river chemistry. *EOS* **98**, 217–218.

McGuire A. D., Anderson L. G., Christensen T. R., Dallimore S., Guo L., Hayes D. J., Heimann M., Lorenson T. D., Macdonald R. W. and Roulet N. (2009) Sensitivity of the carbon cycle in the Arctic to climate change. *Ecol. Monogr.* **79**, 523–555.

Meyers P. A. (1997) Organic geochemical proxies of paleoceanographic, paleolimnologic, and paleoclimatic processes. *Org. Geochem.* **27**, 213–250.

Mook W. G., Bommerson J. C. and Staverman W. H. (1974) Carbon isotope fractionation between dissolved bicarbonate and gaseous carbon dioxide. *Earth Planet. Sci. Lett.* **22**, 169–176.

Norrman B., Zweifel U. L., Hopkinson C. S. and Fry B. (1995) Production and utilization of dissolved organic-carbon during an experimental diatom bloom. *Limnol. Oceanogr.* **40**, 898–907.

Opsahl S., Benner R. and Amon R. M. W. (1999) Major flux of terrigenous dissolved organic matter through the Arctic Ocean. *Limnol. Oceanogr.* **44**, 2017–2023.

Östlund H. G. and Hut G. (1984) Arctic Ocean water mass balance from isotope data. *J. Geophys. Res.* **89**(6373), 81.

Pabi S., van Dijken G. L. and Arrigo K. R. (2008) Primary production in the Arctic Ocean, 1998–2006 RID C-5276-2011. *J. Geophys. Res. Oceans* **113**, C08005.

Peterson B. J. and Fry B. (1987) Stable isotopes in ecosystem studies. *Annu. Rev. Ecol. Syst.* **18**, 293–320.

Pipko I. I., Semiletov I. P., Tishchenko P. Y., Pugach S. P. and Christensen J. P. (2002) Carbonate chemistry dynamics in Bering Strait and the Chukchi Sea. *Prog. Oceanogr.* **55**, 77–94.

Popp B. N., Laws E. A., Bidigare R. R., Dore J. E., Hanson K. L. and Wakeham S. G. (1998) Effect of phytoplankton cell geometry on carbon isotopic fractionation. *Geochim. Cosmochim. Acta* **62**, 69–77.

Quay P. D., Wilbur D. O., Richey J. E., Hedges J. I., Devol A. H. and Victoria R. (1992) Carbon Cycling in the Amazon River - Implications from the C-13 Compositions of Particles and Solutes. *Limnol. Oceanogr* **37**, 857–871.

Rau G. H., Riebesell U. and Wolf-Gladrow D. (1996) A model of photosynthetic C-13 fractionation by marine phytoplankton based on diffusive molecular CO_2 uptake. *Mar. Ecol. Prog. Ser.* **133**, 275–285.

Raymond P. A., McClelland J. W., Holmes R. M., Zhulidov A. V., Mull K., Peterson B. J., Striegl R. G., Aiken G. R. and Gurtovaya T. Y. (2007) Flux and age of dissolved organic carbon exported to the Arctic Ocean: a carbon isotopic study of the five largest arctic rivers. *Global Biogeochem. Cycles* **21**, GB4011.

Roberts K., Granum E., Leegood R. C. and Raven J. A. (2007) C-3 and C-4 pathways of photosynthetic carbon assimilation in marine diatoms are under genetic, not environmental, control. *Plant Physiol.* **145**, 230–235.

Sanchez-Garcia L., Alling V., Pugach S., Vonk J., van Dongen B., Humborg C., Dudarev O., Semiletov I. and Gustafsson O. (2011) Inventories and behavior of particulate organic carbon in the Laptev and East Siberian seas RID H-5422-2011. *Global Biogeochem. Cycles* **25**, GB2007.

Semiletov I. and Gustafsson Ö. (2009) East Siberian Shelf study alleviates scarcity of observations. *Eos Trans. AGU* **90**(17). http://dx.doi.org/10.1029/2009EO170001.

Semiletov I., Dudarev O., Luchin V., Charkin A., Shin K. H. and Tanaka N. (2005) The East Siberian sea as a transition zone between Pacific-derived waters and Arctic shelf waters. *Geophys. Res. Lett.* **32**, L10614.

Semiletov I. P., Pipko I. I., Repina I. and Shakhova N. E. (2007) Carbonate chemistry dynamics and carbon dioxide fluxes across the atmosphere-ice-water interfaces in the Arctic Ocean: Pacific sector of the Arctic. *J. Mar. Syst.* **66**, 204–226.

Shakhova N., Semiletov I. and Gustafsson O. (2010) Methane from the East Siberian Arctic Shelf response. *Science* **329**, 1147–1148.

Schlosser P., Bauch D., Fairbanks R. and Bonisch G. (1994) Arctic river-runoff – mean residence time on the Shelves and in the Halocline. *Deep-Sea Res. Part I. Oceanogr. Res. Pap.* **41**, 1053–1068.

Steele M. and Ermold W. (2004) Salinity trends on the Siberian shelves. *Geophys. Res. Lett.* **31**, L24308.

Stein R. and Macdonald R. W. (2004) *The Organic Carbon Cycle in the Arctic Ocean, vol. 1*. Springer Verlag, Heidelberg, p. 363.

Striegl R. G., Kortelainen P., Chanton J. P., Wickland K. P., Bugna G. C. and Rantakari M. (2001) Carbon dioxide partial pressure and C-13 content of north temperate and boreal lakes at spring ice melt. *Limnol. Oceanogr.* **46**, 941–945.

Tarnocai C., Canadell J. G., Schuur E. A. G., Kuhry P., Mazhitova G. and Zimov S. (2009) Soil organic carbon pools in the northern circumpolar permafrost region. *Global Biogeochem. Cycles* **23**, GB2023.

Torres M. E., Mix A. C. and Rugh W. D. (2005) Precise delta C-13 analysis of dissolved inorganic carbon in natural waters using automated headspace sampling and continuous-flow mass spectrometry. *Limnol. Oceanogr. Methods* **3**, 349–360.

Tortell P. D., Reinfelder J. R. and Morel F. M. M. (1997) Active uptake of bicarbonate by diatoms. *Nature* **390**, 243–244.

van Dongen B. E., Zencak Z. and Gustafsson O. (2008) Differential transport and degradation of bulk organic carbon and specific terrestrial biomarkers in the surface waters of a sub-arctic brackish bay mixing zone. *Mar. Chem.* **112**, 203–214.

Vonk J. E., Sanchez-Garcia L., Semiletov I., Dudarev O., Eglinton T., Andersson A. and Gustafsson O. (2010) Molecular and radiocarbon constraints on sources and degradation of terrestrial organic carbon along the Kolyma paleoriver transect, East Siberian Sea. *Biogeosciences* **7**, 3153–3166.

Waite A. M., Gustafsson O. and Tiselius P. (2005) Linking ecosystem dynamics and biogeochemistry: sinking fractionation of organic carbon in a Swedish fjord. *Limnol. Oceanogr.* **50**(2), 658–671.

Zeebe R. and Wolf-Gladrow D. (2001) *CO_2 in Seawater: Equilibrium, Kinetics, Isotopes*. Elsevier, Amsterdam.

Zhang J., Quay P. D. and Wilbur D. O. (1995) Carbon-isotope fractionation during gas–water exchange and dissolution of CO_2. *Geochim. Cosmochim. Acta* **59**, 107–114.

Associate editor: David J. Burdige